We are IntechOpen,
the world's leading publisher of
Open Access books
Built by scientists, for scientists

4,800
Open access books available

122,000
International authors and editors

135M
Downloads

Our authors are among the

154
Countries delivered to

TOP 1%
most cited scientists

12.2%
Contributors from top 500 universities

CLARIVATE ANALYTICS
BOOK CITATION INDEX
INDEXED

WEB OF SCIENCE™

Selection of our books indexed in the Book Citation Index
in Web of Science™ Core Collection (BKCI)

Interested in publishing with us?
Contact book.department@intechopen.com

Numbers displayed above are based on latest data collected.
For more information visit www.intechopen.com

Two-Phase Flow Boiling
Heat Transfer for Evaporative Refrigerants
in Various Circular Minichannels

Jong-Taek Oh[1], Hoo-Kyu Oh[2] and Kwang-Il Choi[1]
[1]Department of Refrigeration and Air-Conditioning Engineering,
Chonnam National University,
San 96-1, Dunduk-dong, Yeosu, Chonnam 550-749
[2]Department of Refrigeration and Air Conditioning Engineering,
Pukyong National University,
100, Yongdang-dong, Nam-Ku, Busan 608-739,
Republic of Korea

1. Introduction

Global awareness of climate change has been raised in recent decades; many countries proposed to reduce carbon emissions and to control refrigerants based on the Montreal protocol. The ozone layer has become a concern for many researchers, focusing on reducing depletion. Refrigerant has been used for a long time and is still used as the principle material in refrigeration systems. The demand for new methods of refrigeration and air conditioning has promoted more effective and efficient refrigeration systems. Small refrigeration systems might be one of the solutions to reduce depletion of ozone layer indirectly.

Several studies and experimental results have been issued that discussed flow patterns in horizontal tubes, two-phase flow boiling heat transfer and pressure drop using refrigerant as the observed fluid. Two-phase flow boiling heat transfer pressure drop of refrigerants in minichannels has been researched for several decades. Only a few studies in the literature report on the two-phase flow heat transfer and pressure drop of refrigerants in minichannels. Compared with pure refrigerants in conventional channels, the flow boiling of refrigerants in minichannels has discrete characteristics due to the physical and chemical properties of the refrigerants and the dimensions of the minichannels.

The greatest advantages of the minichannels are their high heat transfer coefficients, significant decreases in the size of compact heat exchangers, and lower required fluid mass. A higher heat transfer in minichannels is due to large ratios of heat transfer surface to fluid flow volume and its properties. The decreasing size also allows heat exchangers to achieve significant weight reductions, lower fluid inventories, low capital and installation costs, and energy savings. Despite those advantages, pressure drop within minichannels is higher than that of conventional tube because of the increase of wall friction.

Chisholm (1967) proposed a theoretical basis for the Lockhart–Martinelli correlation for two-phase flow. The Friedel (1979) correlation was obtained by optimizing an equation for the two-phase frictional multiplier using a large measurement database. Many studies have

developed pressure drop correlations on the basis of the Chisholm (1967) and Friedel (1979) correlations. Mishima and Hibiki (1996), Yu et al.(2002), and Kawahara et al. (2002) developed pressure drop correlations on the basis of the Chisholm (1967) correlation.

Chang et al. (2000), Chen et al. (2001), and Zhang and Webb (2001) developed pressure drop correlations on the basis of the Friedel (1979) correlation. Tran et al. (2000) measured the two-phase flow pressure drop with refrigerants R-134a, R-12, and R-113 in small round and rectangular channels. They modified Chisholm's (1983) correlation and proposed a new correlation.

This chapter reports on a study whose goals were to present pressure drop experimental data for the refrigerant R-22, and its alternatives, R-134a, R-410A, R-290, R-717 (NH$_3$) and R-744 (CO$_2$) which were measured in horizontal and local heat transfers during evaporation in smooth minichannels to establish a new correlation for heat exchangers with minichannel designs. The present experimental data for pressure drop were obtained by the previous experiments compared with existing two-phase pressure drop prediction methods, namely Beattie and Whalley (1982), Cicchitti et al (1960), McAdams (1954), Chang et al. (2000), Dukler et al. (1964), Friedel (1979), Chisholm (1983), Tran et al. (2000), Zhang and Webb (2001), Mishima and Hibiki (1996), Lockhart and Martinelli (1949), Shah (1988), Tran et al. (1996), Jung at al. (1989), Gungor and Winterton (1987), Takamatsu et al (1993), Kandlikar and Stainke (2003), Wattelet et al (1994), Chen (1966), Zhang et al. (2004), Chang and Ro (1996), Yu et al. (2002), Friedel (1979), Kawahara et al. (2002), Mishima (1983), Chisholm et al. (2000), Tran et al. (2000), Chen (2001), and Yoon et al. (2004). A new correlation for two-phase frictional pressure drop was developed on the basis of the Lockhart–Martinelli method using the present experimental data. In the present paper, heat fluxes to make the flow boiling heat transfer coefficients were electrically heated. The experimental results were compared with the predictions of seven existing heat transfer correlations, namely those reported by Mishima and Hibiki (1996), Friedel (1979), Chang at al. (2000), Lockhart and Martinelli (1949), Chisholm (1983), Zhang and Webb (2001), Chen (1966), Chen et al. (2001), Kawahara et al. (2002), Tran et al. (1996), Tran et al. (2000), Wattelet et al. (1993), Wattelet et al. (1994), Gungore-Winterton (1986), Gungore-Winterton (1989), Zhang et al (2004), Kandlikare-Steinke (1996), Kandlikare-Steinke (2003), Jung et al.(1989), Jung et al. (2004), Shah (1988), Gungore-Winterton (1987), Zhang et al (1987), and Takamatsu et al. (2003) was and were developed in this study based on superposition, due to the limitations in the correlation for forced convective boiling of refrigerants in small channels.

Compared with conventional channels, evaporation in small channels may provide a higher heat transfer coefficient due to their higher contact area per unit volume of fluid. In evaporation within small channels, as reported by Bao et al. (2000), Zhang et al. (2004), Kandlikare-Steinke (2003), Tran et al. (2000), Pettersen (2004), Park and Hrnjak (2007), Zhao et al. [7], Yun et al. (2005), Yoon et al. (2004), Pamitran et al. (2008), and K.-I. Choi (2009), the contribution of nucleate boiling is predominant and laminar flow appears.

The study that was done by A.S. Pamitran et al (2007) and [a/b]K.-I.Choi et al. (2007), yielded a basic understanding about predicting pressure drop and heat transfer coefficients during refrigerants evaporation in minichannels. The studies have also developed correlations and have been compared with other experimental correlations reported in much available literatures in the area of two-phase boiling heat transfer. The methods of creating correlations have good agreements with the experiment data gathered by using refrigerants as the working fluids.

2. Experimental aspects

2.1 Experimental apparatus and method

Experimental facility for inner diameter 3 and 1.5 mm

The experimental facilities are schematically shown in Fig. 1(a) and (b). The test facilities were constructed by A.S. Pamitran et al. (2007) and K.-I. Choi et al (2007) and consisted of a condenser, a subcooler, a receiver, a refrigerant pump, a mass flow meter, a preheater, and test sections. For the test with 3.0 and 1.5mm inner diameter tubes, a variable AC output motor controller was used to control the flow rate of the refrigerant. A Coriolis-type mass flow meter was installed in a horizontal layout for the test with 1.5 and 3.0mm inner diameter tubes. A preheater or a cooler was installed to control the vapor quality of the refrigerant by heating or condensing the refrigerant before it entered the test section. For evaporation at the test section, a pre-determined heat flux was applied from a variable A.C voltage controller. The vapor refrigerant from the test section was then condensed in the condenser and subcooler, and then the condensed refrigerant was supplied to the receiver.

The test section was made of stainless steel circular smooth tubes with inner tube diameters of 3.0 and, 1.5 mm. The rate of input electric potential E and current I were adjusted in order to control the input power and to determine the applied heat flux, which was measured by a standard multimeter. The test sections were uniformly and constantly heated by applying the electric current directly to their tube walls. The test sections were well insulated with foam and rubber; therefore, heating loss was ignored in the present study. The local saturation pressure of the refrigerant, which was used to determine the saturation temperature, was measured using bourdon tube type pressure gauges with a 0.005 MPa scale at the inlet and at the outlet of the test sections. Differential pressure was measured by the bourdon tube type pressure gauges and a differential pressure transducer. Circular sight glasses with the same inner tube diameter as the test section were installed at the inlet and outlet of the test section to visualize the flow. Each sight glass was held by flanges on both sides, as described in Fig. 1.

The temperature and flow rate measurements were recorded using the Darwin DAQ32 Plus logger R9.01 software program and version 2.41 of the Micro Motion ProLink Software package, respectively. The physical properties of the refrigerants were obtained from the REFPROP 8.0.
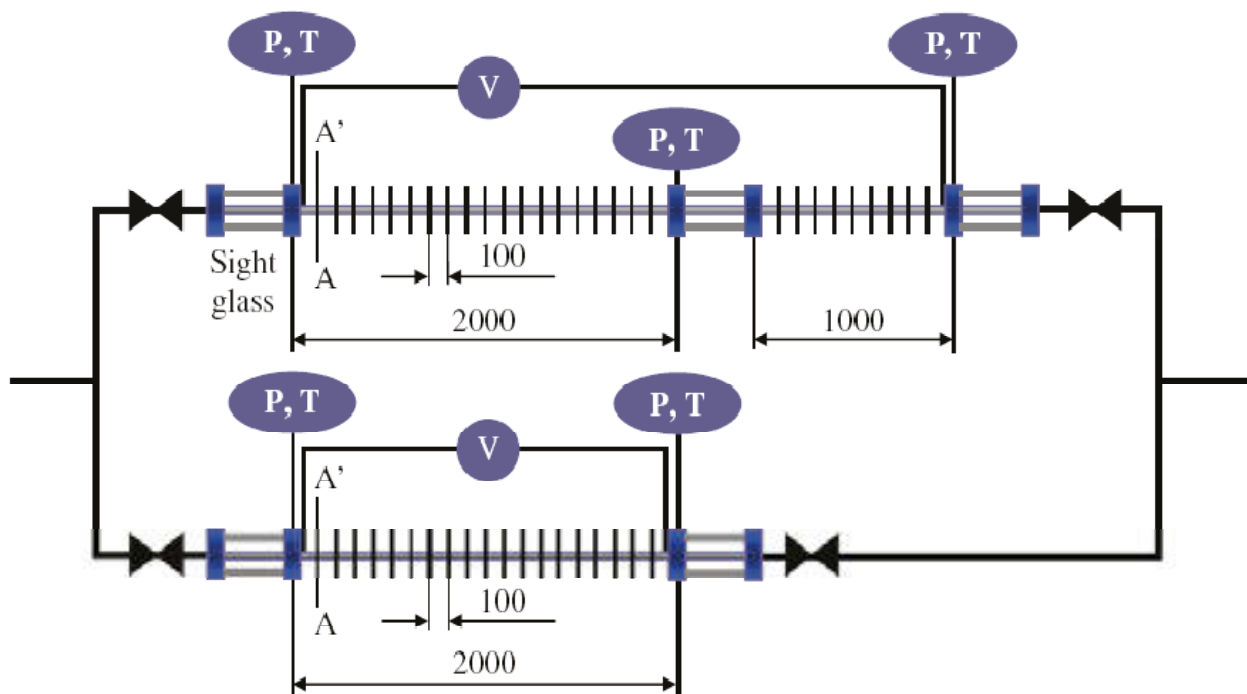
Experimental facility for inner diameter 0.5 mm

Another experimental facility was made for 0.5 mm inner diameter tubes; this facility is an open-loop system. This system allows the refrigerant flow from higher pressure containers to refrigerant receivers. This system used a needle valve to the control flow rate before entering the test section which is made of stainless steel. A weighing balance was used for the test with the 0.5 mm inner diameter tube to measure the refrigerant flow rate. Heating and measurements were similar to those on Fig. 1.

The experimental conditions used in the studies of A.S Pamitran et al and K.-I. Choi et al. are listed in Table 1. Five refrigerants are use as the working fluid in the experiments; the studies express the effects of dimensional factors that are represented by the inner diameter of the tubes. The mass flux effect was observed by configuring the velocity of the fluids and heat flux control by regulating the electrical heating.
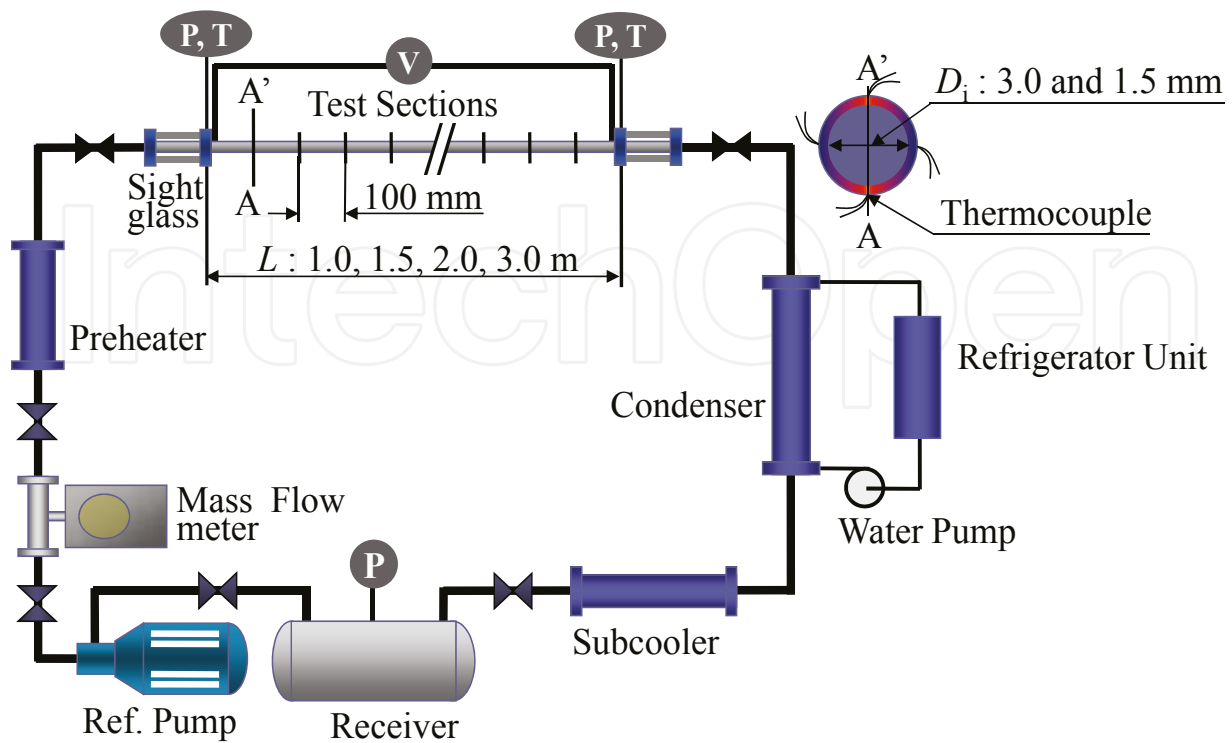
(a)

(b)

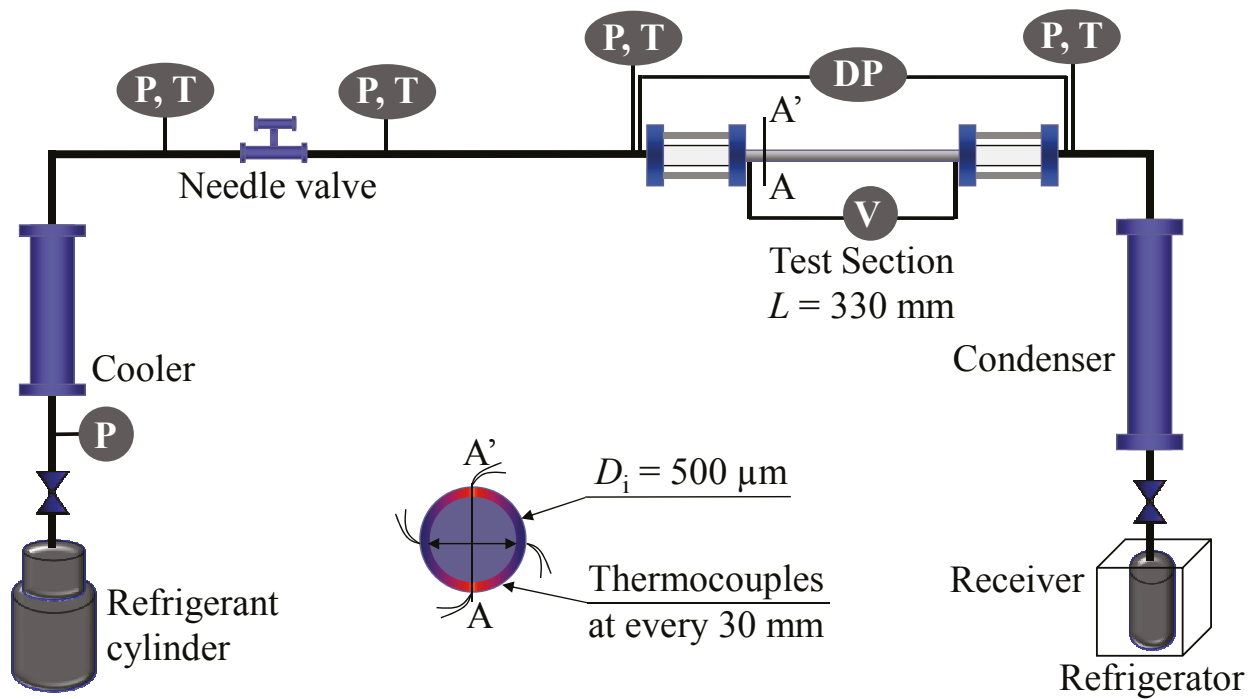Fig. 1. Experimental test facility: (a) for test section with inner tube diameter of D_i=3.0mm and D_i=1.5 mm

Fig. 2. For test section with inner tube diameter of D_i =0.5 mm

Test section	Quality	Working refrigerant	Inner diameter (mm)	Tube length (mm)	Mass flux (kg/(m² ·s))	Heat flux (kW/m²)	Inlet Tsat (°C)
Horizontal circular smooth small tubes	up to 1.0	R-22	3.0	2000	400 – 600	20 – 40	10
			1.5	2000	300 – 600	10 – 20	10
		R-134a	3.0	2000	200 – 600	10 – 40	10
			1.5	2000	200 – 400	10	10
			0.5	330	100	5 – 20	6 – 10
		R-410A	3.0	3000	300 – 600	10 – 40	10 – 15
			1.5	1500	300 – 600	10 – 30	10 – 15
			0.5	330	70 – 400	5 – 20	1 – 11
		C_3H_8	3.0	2000	50 – 240	5 – 25	0 – 11
			1.5	2000	100 – 400	5 – 20	0 – 12
		CO_2	3.0	2000	200 – 600	20 – 30	1 – 10
			1.5	2000	300 – 600	10 – 30	0 – 11
		NH_3	3.0	2000	100 – 800	10 – 70	0 – 10
			1.5	2000	100 – 500	10 – 35	0 – 10

Table 1. Experiment conditions

The experimental uncertainty associated with all the parameters is tabulated in Table 2. The uncertainties were obtained using both random and systematic errors, and these uncertainty values changed according to the flow conditions; their minimum to maximum ranges are shown.

Parameters	Uncertainty (%)				
	CO_2	C_3H_8	R-410A	R-134a	R-22
T_{wi} (%)	±2.10 to ±4.56	±0.18 to ±5.58	±0.23 to ±6.53	±0.29 to ±3.92	±0.44 to ±3.90
P (kPa)	±2.5 kPa	±2.5 kPa	±2.5 kPa	±2.5 kPa	±2.5 kPa
G(%)	±1.85 to ±9.48	±3.24 to ±9.78	±1.84 to ±9.48	±1.85 to ±3.80	±1.84 to ±3.16
q(%)	±1.67 to ±2.70	±2.07 to ±3.58	±1.67 to ±3.20	±1.79 to ±2.59	±1.78 to ±2.26
x(%)	±1.79 to ±9.71	±4.27 to ±9.82	±1.78 to ±9.85	±2.23 to ±4.19	±1.88 to ±3.39
h(%)	±4.46 to ±8.23	±1.78 to ±9.89	±2.59 to ±10.33	±2.75 to ±9.24	±2.74 to ±9.07

Table 2. Summary of estimated uncertainty

3. Data reduction

3.1 Pressure drop

The saturation pressure at the initial point of saturation was determined by interpolating the measured pressure and the subcooled length. The experimental two-phase frictional pressure drop can be obtained by subtracting the calculated acceleration pressure drop from the measured pressure drop.

$$\left(\frac{dp}{dz}\right) = \left(\frac{dp}{dz}F\right) + \left(\frac{dp}{dz}a\right) + \left(\frac{dp}{dz}z\right) \tag{1}$$

$$-\left(\frac{dp}{dz}a\right) = G^2 \frac{d}{dz}\left(\frac{x^2 v_g}{\alpha} + \frac{(1-x)^2 v_f}{(1-\alpha)}\right) \tag{2}$$

$$-\left(\frac{dp}{dz}z\right) = g\sin\theta\left[\frac{A_g}{A}\rho_g + \frac{A_f}{A}\rho_g\right] = g\sin\theta[\alpha\rho_g + (1-\alpha)\rho_f] \tag{3}$$

The equation for the friction pressure gradient for horizontal tubes should be reduced to the static head factor, therefore the equation is

$$\left(\frac{dp}{dz}F\right) = \left(\frac{dp}{dz}\right) - \left(\frac{dp}{dz}a\right) = \left(\frac{dp}{dz}\right) - G^2 \frac{d}{dz}\left(\frac{x^2}{\alpha\rho_g} + \frac{(1-x)^2}{(1-\alpha)\rho_f}\right) \tag{4}$$

The predicted void fraction with Steiner (1993), CISE (Premoli et al., 1971) and Chisholm (1972) are compared in the present study, as is shown in Fig. 3. The absolute deviations of the Steiner (1993), CISE (Premoli et al., 1971) and Chisholm (1972) void fractions from the homogenous void fraction are 7.11%, 3.72% and 11.49%, respectively. The predicted pressure drop for the present experimental data using some previous pressure drop correlations with the Steiner (1993) void fraction showed a better prediction than that using the CISE (Premoli et al., 1971) and Chisholm (1972) void fractions. Therefore, the void fraction in the present study was obtained from the Steiner (1993) void fraction.

$$\alpha = \frac{x}{\rho_g}\left[(1 + 0.12(1 - x))\left(\frac{x}{\rho_g} + \frac{(1 - x)}{\rho_f}\right) + \left(\frac{1.18}{G^2}\right)\left(\frac{(1 - x)}{\rho_f^{0.5}}\right)\left(g\sigma(\rho_f + \rho_g)\right)^{0.25}\right]^{-1} \quad (5)$$

The friction factor was determined from the measured pressure drop for a given mass flux by using the Fanning equation

$$f_{tp} = \frac{D\bar{\rho}}{2G^2}\left(-\frac{dp}{dz}F\right) \quad (6)$$

where the average density is calculated with the following equation:

$$\bar{\rho} = \alpha\rho_g + (1 + \alpha)\rho_f \quad (7)$$

In order to obtain the two-phase frictional multiplier based on the pressure drop for the total flow assumed for the liquid, ϕ_{fo}^2, the calculated two-phase frictional pressure drop is divided by the calculated frictional two-phase pressure drop assuming the total flow to be liquid, as shown by

$$\phi_{fo}^2 = \frac{\left(-\frac{dp}{dz}F\right)_{tp}}{\left(-\frac{dp}{dz}F\right)_{fo}} = \frac{\left(-\frac{dp}{dz}F\right)_{tp}}{\left(-\frac{2f_{fo}G^2}{D\rho_f}F\right)} \quad (8)$$
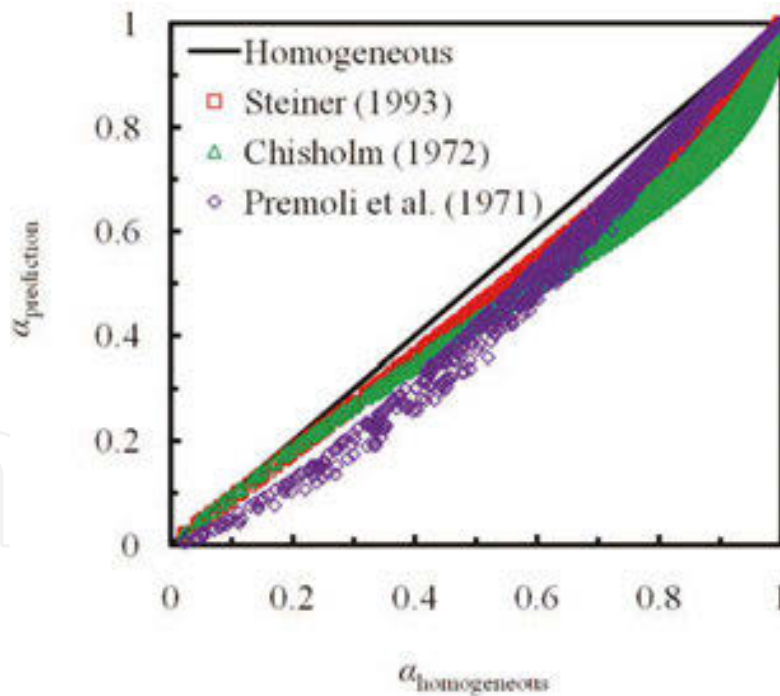
Fig. 3. Void fraction comparison

3.2 Heat transfer coefficient
The inside tube wall temperature, T_{wi} was the average temperature of the top, both right and left sides, and bottom wall temperatures, and was determined using steady-state one-dimensional radial conduction heat transfer through the wall with internal heat generation.

The quality, x, at the measurement locations, z, were determined based on the thermodynamic properties, namely,

$$x = \frac{i - i_f}{i_{fg}} \tag{9}$$

The refrigerant flow at the inlet of the test section was not completely saturated. Even though it was just short of being completely saturated, it was necessary to determine the subcooled length to ensure reduction data accuracy. The subcooled length was calculated using the following equation to determine the initial point of saturation.

$$z_{sc} = L \frac{i_f - i_{fi}}{\Delta i} = L \frac{i_f - i_{fi}}{(Q/W)} \tag{10}$$

The outlet mass quality was then determined using the following equation:

$$x = \frac{\Delta i + i_{fg} - i_f}{i_{fg}} \tag{11}$$

4. Results and discussion

The flow with heat addition, or adiabatic flow, is a coupled thermodynamic problem. On the one hand, heat transfer leads to a phase change, which leads to the change of phase distribution and flow pattern; on the other hand, it causes a change in the hydrodynamics, such as the pressure drop along the flow path, which affects the heat transfer characteristics. Furthermore, a single-component, two-phase flow in a tube can hardly become fully developed at low pressure because of the shape change in large bubbles and the inherent pressure change along the tube, which continually changes the state of the fluid and thereby changes the phase distribution and flow pattern. The current study presents the characteristics of a two-phase flow pattern and pressure drop in small tubes for some refrigerants.

4.1 Flow pattern

The hydrodynamic characteristic of two-phase flows, such as the pressure drop, void fraction, or velocity distribution, varies systematically with the observed flow pattern, just as in the case of a single-phase flow, whose behavior depends on whether the flow is in the laminar or turbulent regime. However, in contrast to a single-phase flow, liquid–vapor flows are difficult to describe by general principles, which could serve as a framework for solving practical work. The identification of a flow regime provides a picture of the phase boundaries.

The present experimental results were mapped on Wang et al. (1997) and Wojtan et al. (2005) flow pattern maps, which were developed for diabatic two-phase flows. The Wang et al. (1997) flow pattern map is a modified Baker (1954) map, developed using R-22, R-134a, and R-407C inside a 6.5mm horizontal smooth tube. Therefore, they claim that their flow pattern map is better for prediction of flow patterns in small tubes. The Wang et al. (1997) study showed that the flow transition for a mixture refrigerant showed a considerable delay compared with that of pure refrigerants. For R-410A, at the initial stage of evaporation, R-32 evaporated faster than R- 125. Therefore, R-32 increased the concentration of the vapor

phase, and R-125 increased the concentration of the liquid phase throughout the evaporation process at the liquid–vapor interface. This resulted in a higher mean vapor velocity and a lower mean liquid velocity during evaporation. For the other working refrigerants, the physical properties of the refrigerant such as density, viscosity and surface tension have a strong effect on the flow pattern.

The predicted flow pattern for the selected current experimental data according to the existing flow pattern maps of Wojtan et al. (2005) and Wang et al. (1997) can be seen in Figs. 4(a) - (f) and 5(a) – (f), respectively. The Wang et al. (1997) map showed a better prediction of the flow pattern of the current experimental data for the beginning of annular flow than the Wojtan et al. (2005) map; however, the Wang et al. (1997) map could not show the prediction for dry-out conditions. The flow pattern prediction of the current test results for the all test conditions with the Wang et al. (1997) flow pattern map was for the intermittent, stratified wavy and annular flow. The stratified wavy flow appeared earlier for higher mass fluxes and its regime was longer for the low mass flux condition. The annular flow appeared earlier for higher mass fluxes.

The Wojtan et al. (2005) flow pattern map is a modified Kattan et al. (1998) map, developed using R-22 and R-410A inside a 13.6mm horizontal smooth tube. Kattan et al. (1998) used five refrigerants R-134a, R-123, R-402A, R-404A, and R-502 inside 12mm and 10.92mm (only for R-134a) tubes, which were heated by hot water flowing counter-currently to develop their flow pattern maps on the basis of the Steiner (1993) flow pattern map. The flow pattern prediction of the experimental results for all the test conditions with the Wojtan et al. (2005) flow pattern map was on intermittent, annular, dry-out, and mist flows. The flow pattern prediction, as shown in Fig. 4(b)–(c), showed that the mass flux, heat flux and inner diameter had an effect on the flow-pattern. Since the Wojtan et al. (2005) map was developed using a conventional tube, the flow pattern transition of the present experimental data showed a delay on this map. However, the Wojtan et al. (2005) map could predict the dry-out condition. The Wojtan et al. (2005) map predicts the dry-out condition of the R-410A experimental data better than those of the other working refrigerants. Overall, the Wang et al. (1997) flow pattern map provides a better flow pattern prediction for the current experimental results than the Wojtan et al. (2005) flow pattern map.
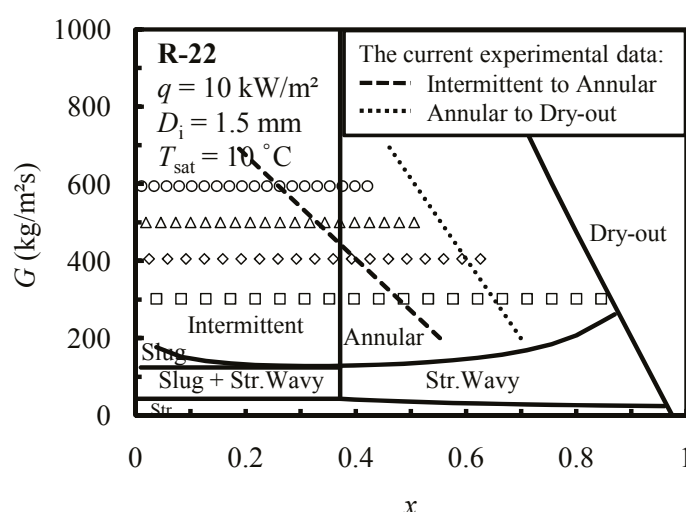

Fig. 4. (a) Present experimental results mapped on Wojtan et al. (2005) flow pattern map for R-22 at q = 10 kW/m², D_i = 1.5 mm, T_{sat} = 10°C
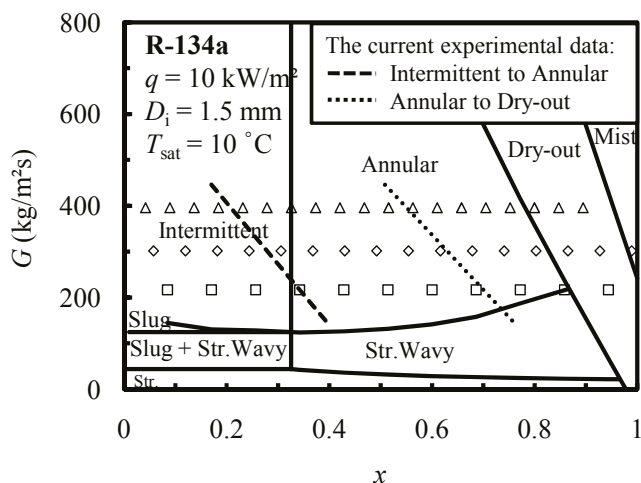
Fig. 4. (b) Present experimental results mapped on Wojtan et al. (2005) flow pattern map for R-134a at q = 10 kW/m², D_i = 1.5 mm, T_{sat} = 10°C
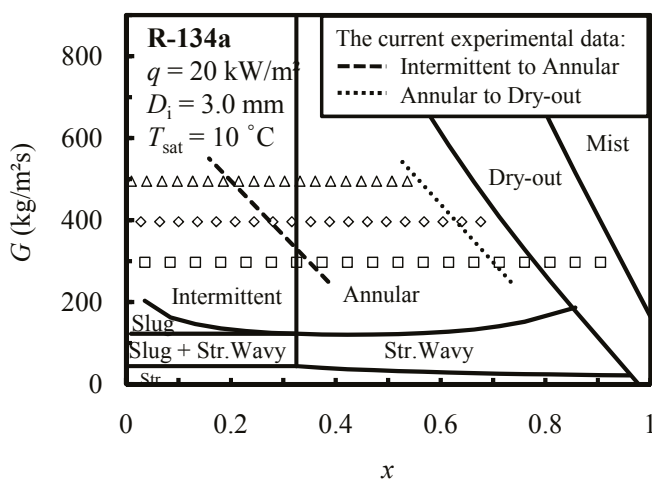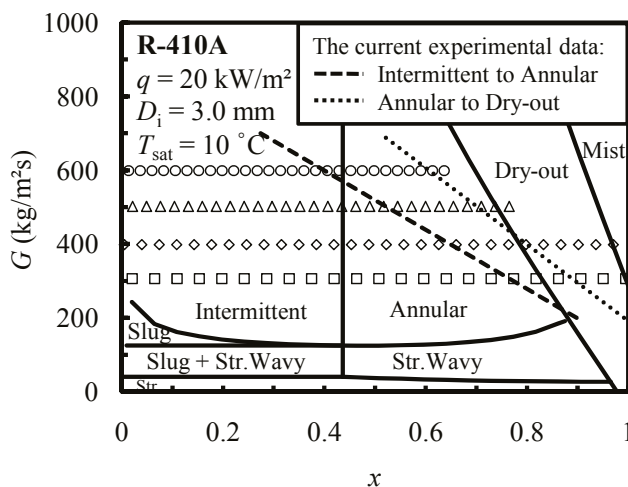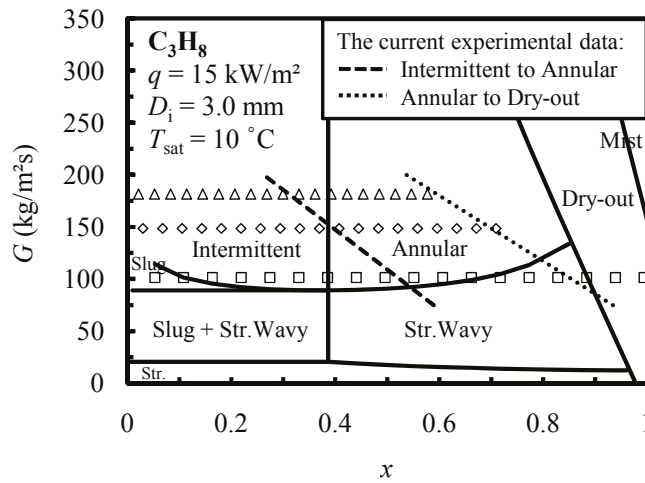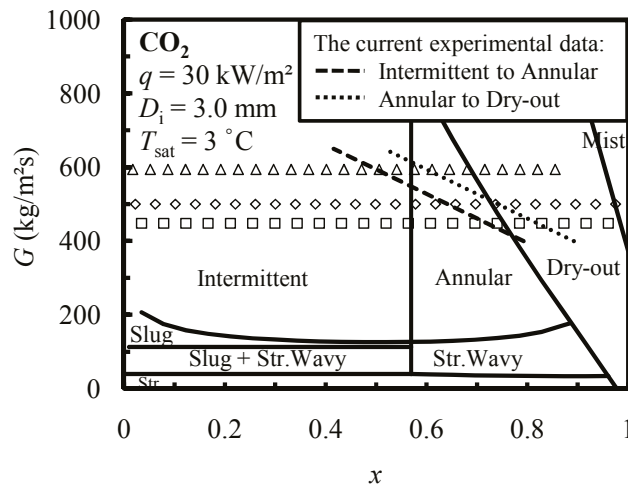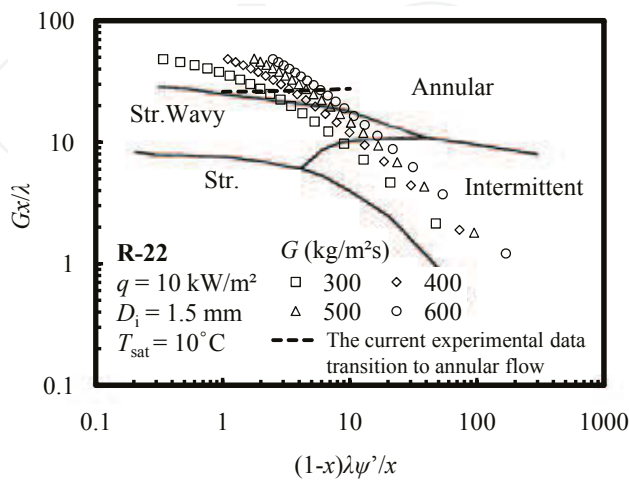

Fig. 4. (c) Present experimental results mapped on Wojtan et al. (2005) flow pattern map for R-134a at q = 20 kW/m², D_i = 3.0 mm, T_{sat} = 10°C

Fig. 4. (d) Present experimental results mapped on Wojtan et al. (2005) flow pattern map for R-410A at q = 20 kW/m², D_i = 3.0 mm, T_{sat} = 10°C

Fig. 4. (e) Present experimental results mapped on Wojtan et al. (2005) flow pattern map for C_3H_8 at $q = 15$ kW/m², $D_i = 3.0$ mm, $T_{sat} = 10°C$

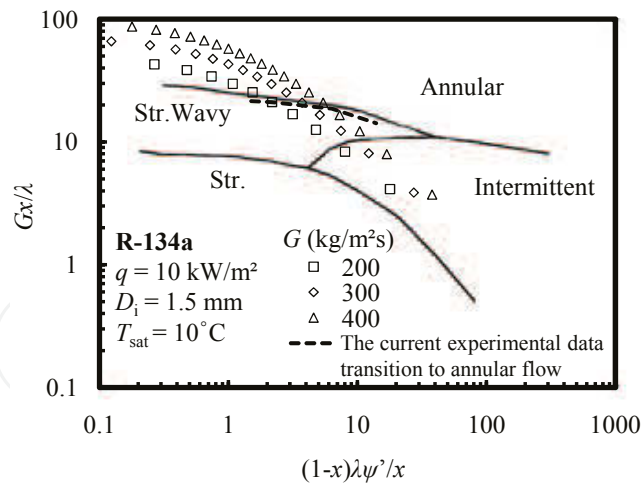Fig. 4. (f) Present experimental results mapped on Wojtan et al. (2005) flow pattern map for CO_2 at $q = 30$ kW/m², $D_i = 3.0$ mm, $T_{sat} = 3°C$

Fig. 5. (a) Present experimental results mapped on Wang et al. (1997) flow pattern map for R-22 at $q = 10$ kW/m², $D_i = 1.5$ mm, $T_{sat} = 10°C$

Fig. 5. (b) Present experimental results mapped on Wang et al. (1997) flow pattern map for R-134a at q = 10 kW/m², D_i = 1.5 mm, T_{sat} = 10°C
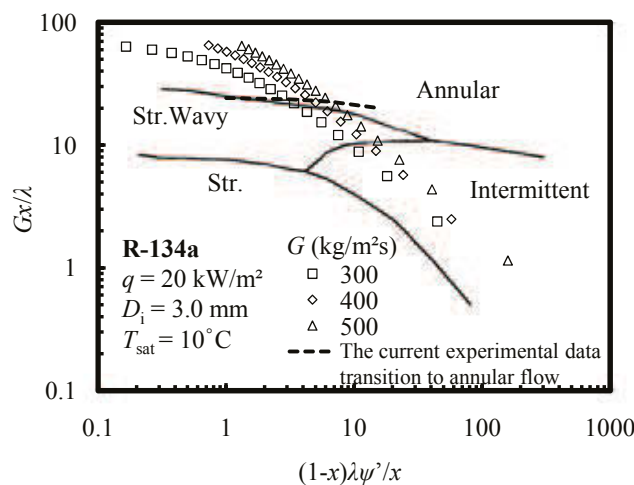

Fig. 5. (c) Present experimental results mapped on Wang et al. (1997) flow pattern map for R-134a at q = 20 kW/m², D_i = 3.0 mm, T_{sat} = 10°C
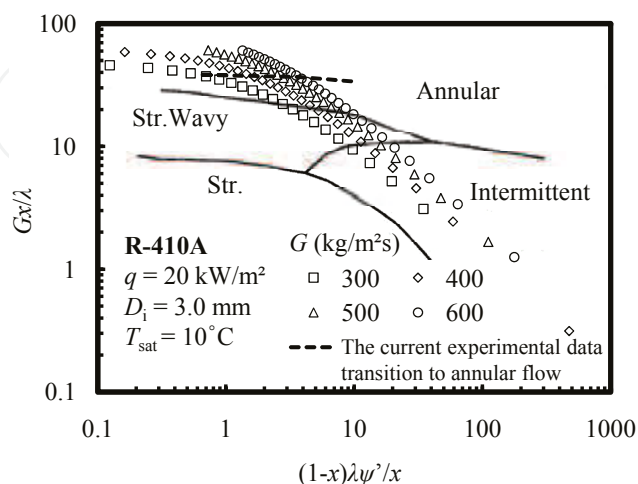

Fig. 5. (d) Present experimental results mapped on Wang et al. (1997) flow pattern map for R-410A at q = 20 kW/m², D_i = 3.0 mm, T_{sat} = 10°C
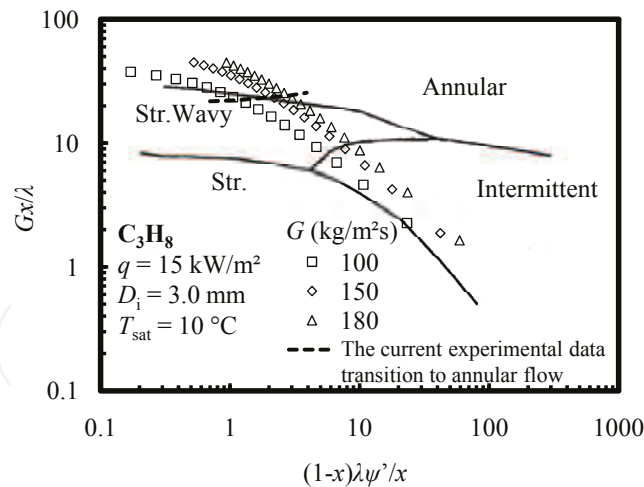
Fig. 5. (e) Present experimental results mapped on Wang et al. (1997) flow pattern map for C_3H_8 at q = 15 kW/m², D_i = 3.0 mm, T_{sat} = 10°C
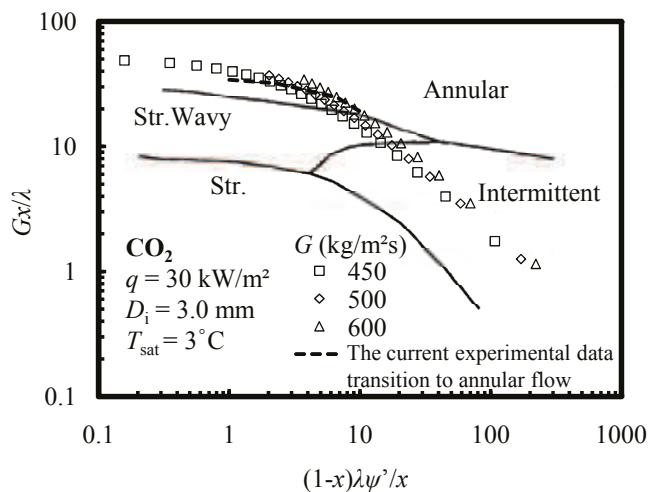

Fig. 5. (f) Present experimental results mapped on Wang et al. (1997) flow pattern map for CO_2 at q = 30 kW/m², D_i = 3.0 mm, T_{sat} = 3°C
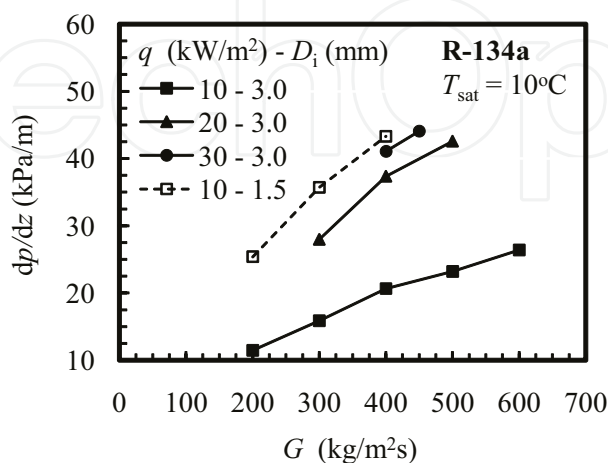
4.2 Pressure drop

Fig. 6(a)-(f) shows that mass flux has a strong effect on the pressure drop. An increase in the mass flux results in a higher flow velocity, which increases the friction and acceleration pressure drops. This similar trend is shown by Zhao et al. (2000), Yoon et al. (2004), Park and Hrnjak (2007), Oh et al. (2008) and Cho and Kim (2007). Fig. 6 also illustrates that the pressure drop increases as the heat flux increases. It is presumed that the increasing heat flux results in a higher vaporization, which increases the average fluid vapor quality and flow velocity; this trend is similar to that shown by Zhao et al. (2000). The effect of the inner tube diameter on the pressure drop is also illustrated in Fig. 6(a)-(f). The pressure gradient in the 1.5 mm tube is higher than that in the 3.0mm tube. The explanation for this is that the smaller inner tube diameter results in a higher wall shear stress, wherein for a given temperature condition it results in a higher friction factor and flow velocity, and then results in both higher frictional and acceleration pressure drops.
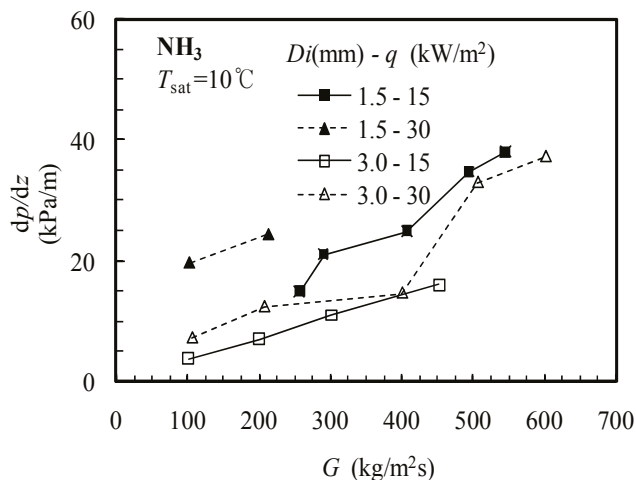
(a) Effect of mass flux, heat flux and inner diameter on pressure drop for NH_3 at T_{sat} = 10°C
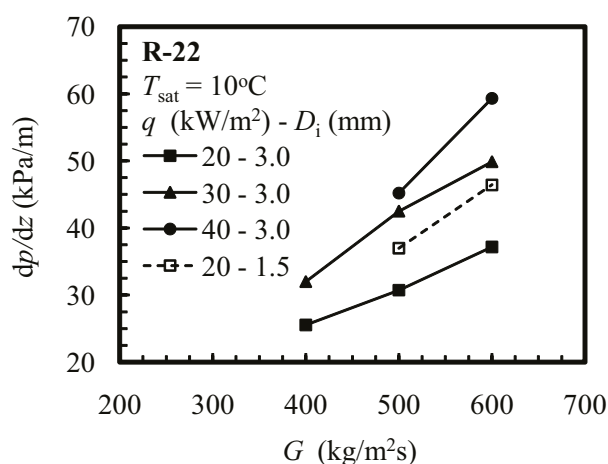
(b) Effect of mass flux, heat flux and inner tube diameter on pressure drop for R-22 at T_{sat} = 10°C

(c) Effect of mass flux, heat flux and inner tube diameter on pressure drop for R-134a at T_{sat} = 10°C

(d) Effect of mass flux, heat flux and inner tube diameter on pressure drop for R-410A at T_{sat} = 10°C

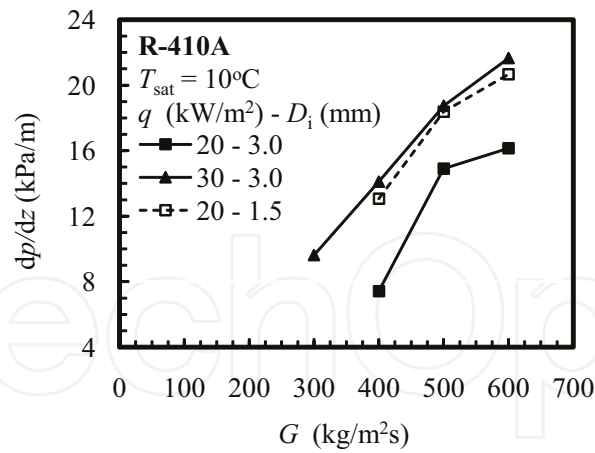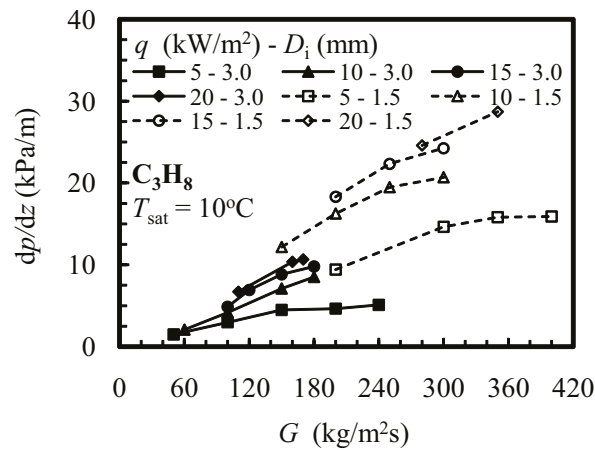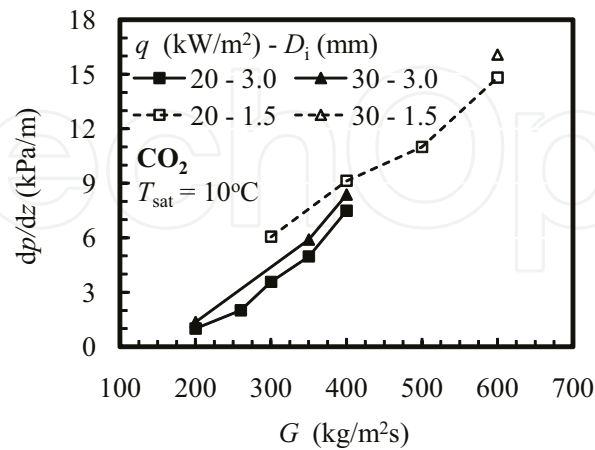(e) Effect of mass flux, heat flux and inner tube diameter on pressure drop for C_3H_8 at T_{sat} = 10°C

(f) Effect of mass flux, heat flux and inner tube diameter on pressure drop for CO_2 at T_{sat} = 10°C

Fig. 6. (a)-(f) The effects of mass flux, heat flux, inner tube diameter, and saturation temperature on pressure drop

Fig. 6 also depicts the effect of saturation temperature on pressure drop, where a lower saturation temperature results in a higher pressure drop. This can be explained by the effect of the physical properties of density and viscosity on the pressure drop at different temperatures. The liquid density, ρ_f, and liquid viscosity, μ_f, increase as the temperature decreases, whereas the vapor density, ρ_g, and vapor viscosity, μ_g, decrease as the temperature decreases. As the temperature decreases for a constant mass flux condition, the increasing liquid density and liquid viscosity result in a lower liquid velocity, whereas the decreasing vapor density and vapor viscosity are the result in a higher vapor velocity. It is clear that the pressure drop increases during evaporation, and this increasing of the pressure drop is higher when the saturation temperature is lower.
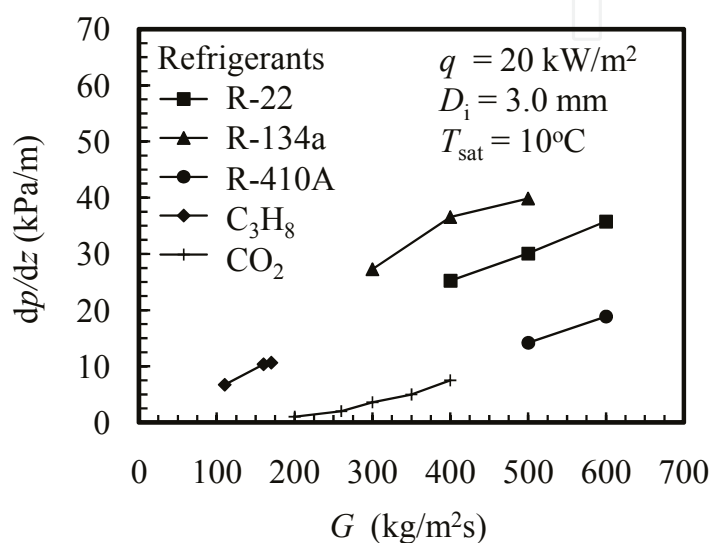
(a) Pressure drop comparison of the present working refrigerants at $q = 20 \text{ kW/m}^2$, $D_i = 3.0$ mm, $T_{sat} = 10°C$
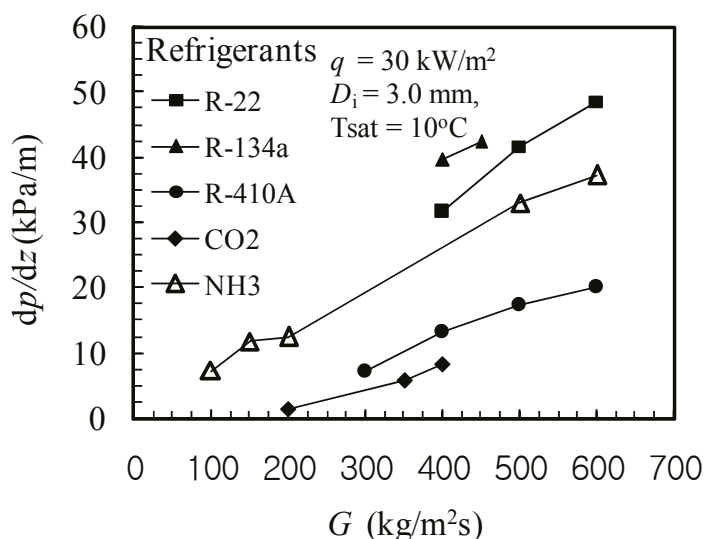
(b) Pressure drop comparison of the present working refrigerants at $q = 30 \text{ kW/m}^2$, $D_i = 3.0$ mm, $T_{sat} = 10°C$

Fig. 7. Pressure drop comparison of the present working refrigerants

The pressure drop of the present working refrigerants is compared under several of the same experimental conditions. The pressure drop comparisons are illustrated in Fig. 7. The order of the pressure drop from the highest to the lowest is R-134a, R-22, NH_3, C_3H_8, R-410A, and CO_2. The pressure drop is strongly affected by the physical properties of the working fluid such as density, viscosity, surface tension and pressure. As shown in Table 3, the working refrigerant with a higher pressure drop has a higher density ratio ρ_f/ρ_g, viscosity ratio μ_f/μ_g, surface tension, and a lower pressure, generally. Therefore, it is clear that in the present comparison that CO_2 has the lowest pressure drop, making CO_2 an effective future environmental friendly refrigerant

Refrigerant	T (°C)	σ (10-3 N/m)	$\mu f/\mu g$	μ_g (10-6 Pa s)	μ_f (10-6 Pa s)	$\rho f/\rho g$	ρ_g (kg/m³)	ρ_f (kg/m³)	P (MPa)
R-22		10.22	16.36	11.96	195.7	43.27	28.82	1247	0.681
R-134a		10.14	21.42	11.15	238.8	62.33	20.23	1261	0.415
R-410A	10	7.16	11.36	12.91	146.6	27.07	41.74	1130	1.085
C_3H_8		8.85	13.96	8.15	113.8	37.32	13.8	515	0.636
CO_2		2.77	5.59	15.46	86.37	6.41	134.4	861.7	4.497
NH_3		29.59	16.35	9.36	153.03	128.32	4.89	623.64	0.615
R-22		10.95	17.62	11.73	206.7	50.99	24.79	1264	0.584
R-134a		10.84	23.25	10.94	254.4	74.61	17.13	1278	0.35
R-410A	5	7.9	12.38	12.6	156	32.21	35.73	1151	0.934
C_3H_8		9.48	15.03	7.97	119.8	43.57	11.98	522	0.551
CO_2		3.64	6.46	14.83	95.84	7.85	114.1	896.7	3.965
NH_3		31.24	17.51	9.21	161.23	153.52	4.115	631.66	0.515

Table 3. Physical properties of R-22, R-134a, R-410A, C_3H_8, CO_2 and NH_3 at 10 and 5°C
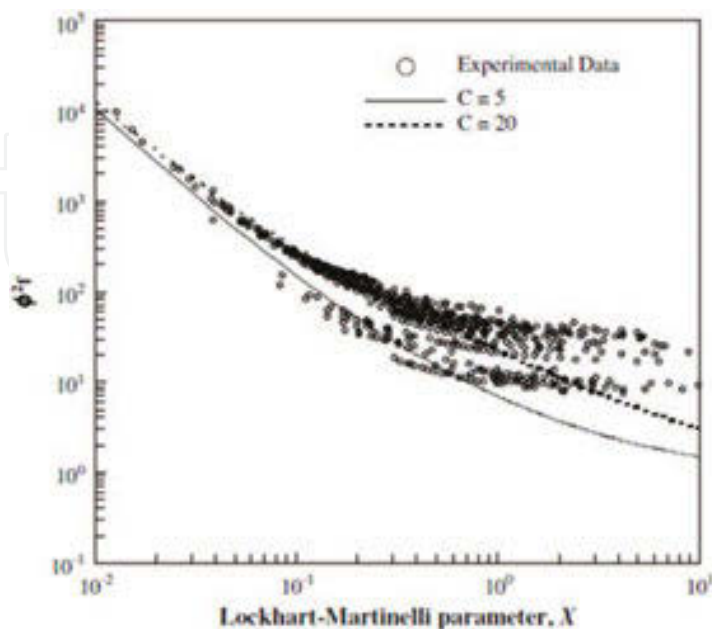
(a) Propane
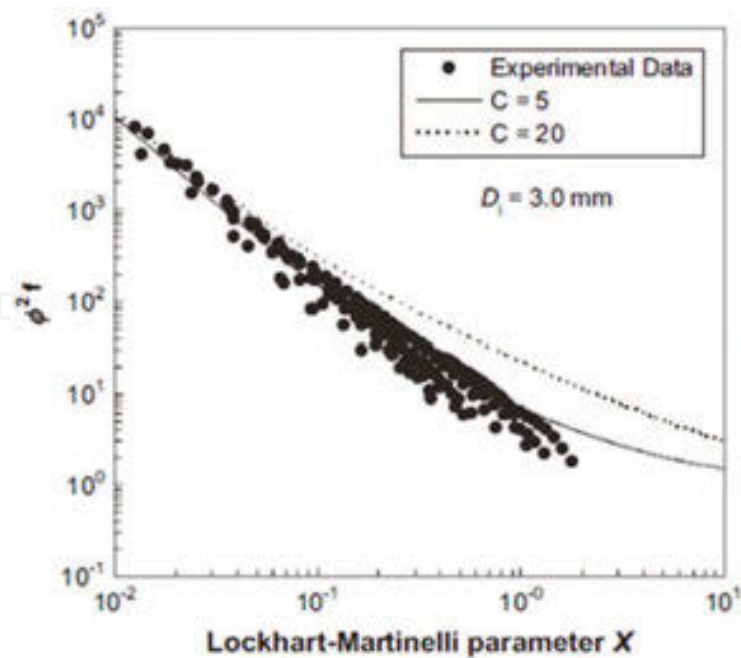
(b) R-410A
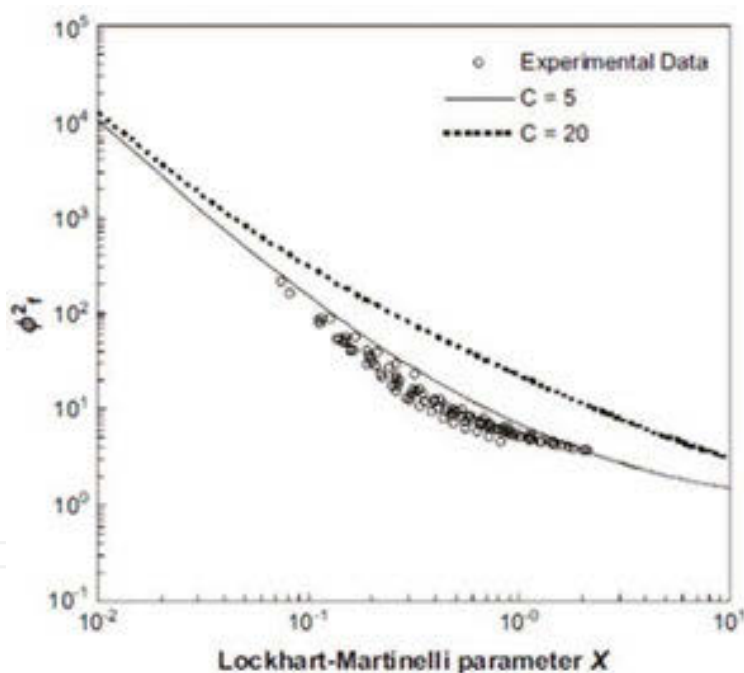
(c) CO$_2$

Fig. 8. Variation of the two-phase frictional multiplier data with the Lockhart–Martinelli parameter., (a) Propane, (b) R-410A and (c) CO$_2$

Fig. 8 (a)-(c) shows a comparison of the two-phase frictional multiplier data with the values predicted by the Lockhart–Martinelli correlation with C= 5 and C= 20, where the Cs are taken from Chisholm (1967). The figure shows that the present data are at the upper the baseline of C = 20, between the baseline of C = 20 and C = 5, and under the baseline of C = 5, which means that laminar, turbulent and the co-current laminar–turbulent flows exist in the present data.

	Previous correlations	**Mean deviation(%)**	**Average deviation(%)**
A.S. Pamitran et al. (2010)	Beattie and Whalley (1982)	23.35	15.91
	Cicchitti et al (1960)	23.51	2.9
	McAdams (1954)	25.25	21.75
	Chang et al. (2000)	26.41	22.65
	Dukler et al. (1964)	27.03	25.37
	Friedel (1979)	28.87	16.44
	Chisholm (1983)	34.65	3.89
	Tran et al. (2000)	42.48	33.05
	Zhang and Webb (2001)	49.04	22.4
	Mishima and Hibiki (1996)	50.71	39.89
	Lockhart and Martinelli (1949)	107	97.69
K.-I. Choi et al. (2009)	Mishima and Hibiki (1996)	35.37	25.08
	Friedel (1979)	38.79	21.91
	Chang at al. (2000)	38.86	21.99
	Lockhart and Martinelli (1949)	41.36	3.46
	Chisholm (1983)	45.24	18
	Zhang and Webb (2001)	46.82	7.58
	Chen et al. (2001)	63.67	63.6
	Kawahara et al. (2002)	73.04	72.92
	Tran et al. (2000)	77.99	35.6
	Homogeneous (Cicchitti et al., 1960)	48.67	-40.27
	Homogeneous (Beattie and Whalley, 1982)	54.68	-51.69
	Homogeneous (Mc Adam, 1954)	56.07	-53.73
	Homogeneous ((Dukler et al., 1964)	58.75	-57.32
K.-I. Choi et al. (2008)	Chang and Ro (1996)	19.57	7.43
	Homogeneous (Beattie and Whalley, 1982)	20.04	7.73
	Homogeneous (Mc Adam, 1954)	20.08	13.31
	Homogeneous (Cicchitti et al., 1960)	20.12	8.11
	Homogeneous ((Dukler et al., 1964)	21.87	18.08
	Yu et al. (2002)	27.14	17.88
	Chen et al(2001)	29.85	7.25
	*Chen et al(2001)	14.4	1.43
	Zhang and Webb (2001)	30.82	30.77
	Friedel (1979)	39.21	39.18
	Chang et al. (2000)	39.43	39.41
	Kawahara et al. (2002)	44.63	44.63
	Mishima (1983)	67.81	66.11
	Chisholm et al. (2000)	98.54	97.25
	Tran et al. (2000)	133.97	133.97
	Lockhart and Martinelli (1949)	145.44	144.58

	Previous correlations	**Mean deviation(%)**	**Average deviation(%)**
A.S. Pamitran et al. (2007)	Homogeneous (Dukler et al. (1964))	18.14	1.63
	Homogeneous (McAdams (1954))	18.33	0.53
	Homogeneous (Beattie and Whalley, 1982)	21.16	12.83
	Homogeneous (Cicchitti et al., 1960)	24.82	14.78
	Kawahara et al. (2002)	30.8	30.43
	Zhang and Webb (2001)	34.3	21.28
	Yu et al. (2002)	48.23	4.33
	Friedel (1979)	68.56	67.89
	Chang et al. (2000)	68.72	68.06
	Yoon et al. (2004)	101.18	93.59
	Chisholm (1983)	101.55	100.24
	Chen et al. (2001)	122.13	122.13
	Tran et al. (2000)	179.57	179.57

Table 4. Deviation of the pressure drop comparison with some existing correlations.

The current experimental two-phase pressure drop data were compared with the predictions from eleven existing correlations. The deviations from the correlation results from the previous experimental data are listed in Table 4, and the selected comparison figures are shown in figures 9(a)-(j). The pressure drop homogenous model of Beattie and Whalley (1982) provided the best prediction in the A.S. Pamitran et al. (2010) study among the other methods, yielding a mean deviation of around 23%. Mishima and Hibiki (1996) is the best correlation to predict the pressure drop in K.-I Choi et al. (2009) with a mean deviation about 35%. The other presented homogenous models also provided relatively good predictions.

Fig. 9. (a) Comparison between the experimental data and the prediction pressure drop with Fridel (1979) correlation

Fig. 9. (b) Comparison between the experimental data and the prediction pressure drop with Cicchitti et al (1960) correlation

Fig. 9. (c) Comparison between the experimental data and the prediction pressure drop with Zang-Webb (2001) correlation

Fig. 9. (d) Comparison between the experimental data and the prediction pressure drop with Chisholm (1983) correlation

Fig. 9. (e) Comparison between the experimental data and the prediction pressure drop with Beattie-Whalley (1982) correlation
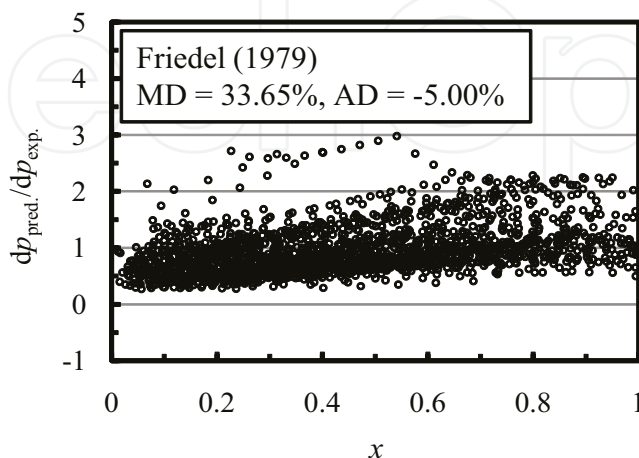

Fig. 9. (f) Comparison between the experimental data and the prediction pressure drop with Chang-Ro (1996) correlation

Fig. 9. (g) Comparison between the experimental data and the prediction pressure drop with Dukler et al. (1964) correlation
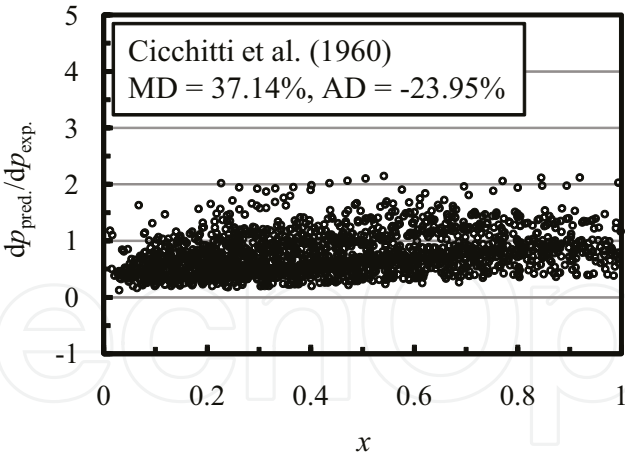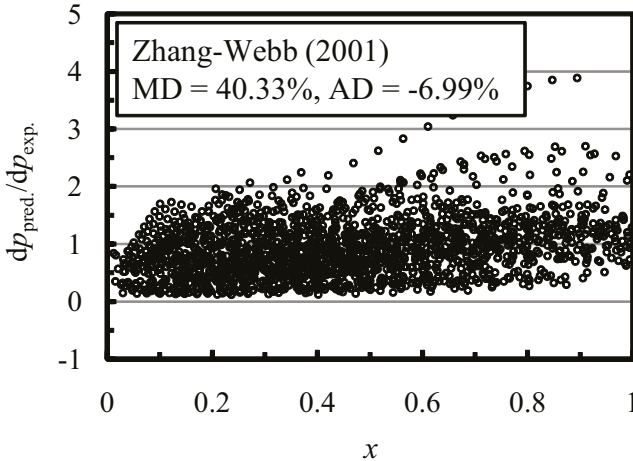
Fig. 9. (h) Comparison between the experimental data and the prediction pressure drop with Trans et al. (2000) correlation
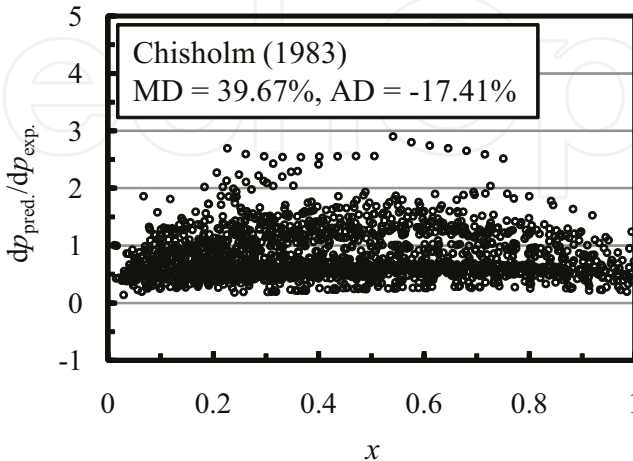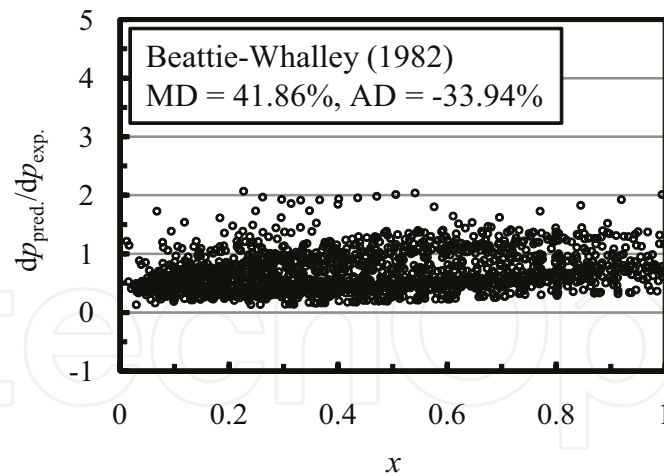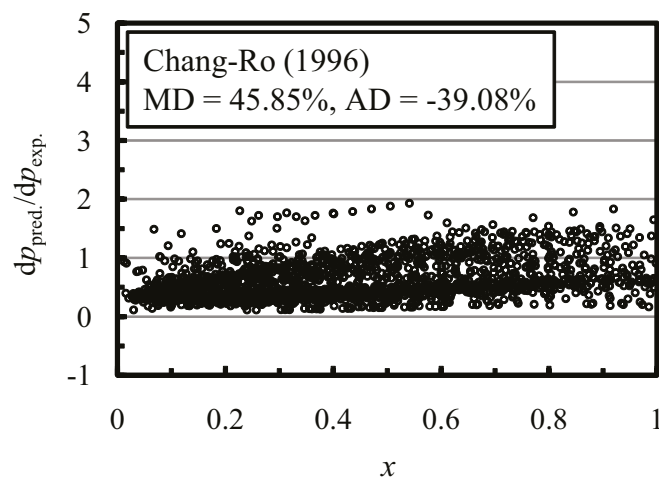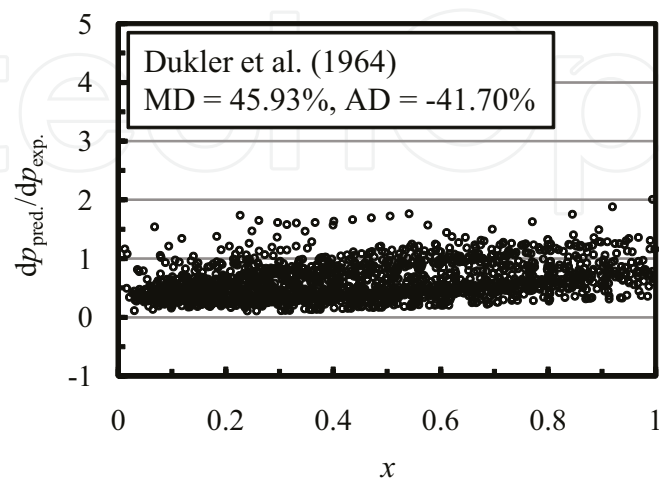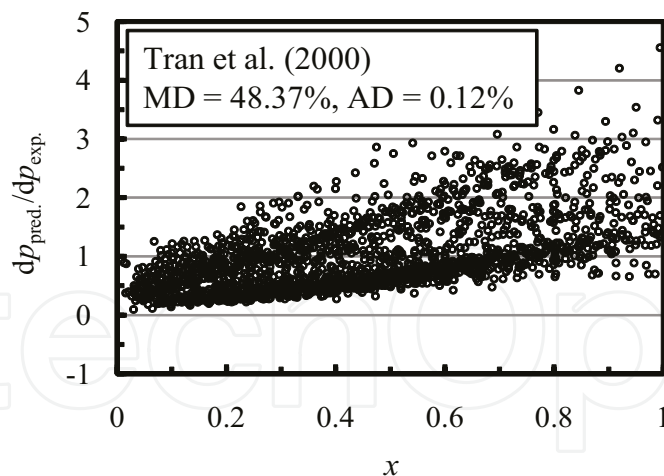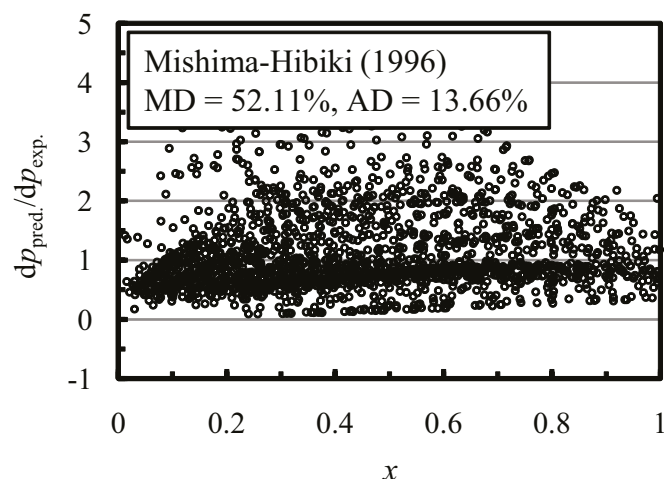

Fig. 9. (i) Comparison between the experimental data and the prediction pressure drop with Mishima – Hibiki (1996) correlation
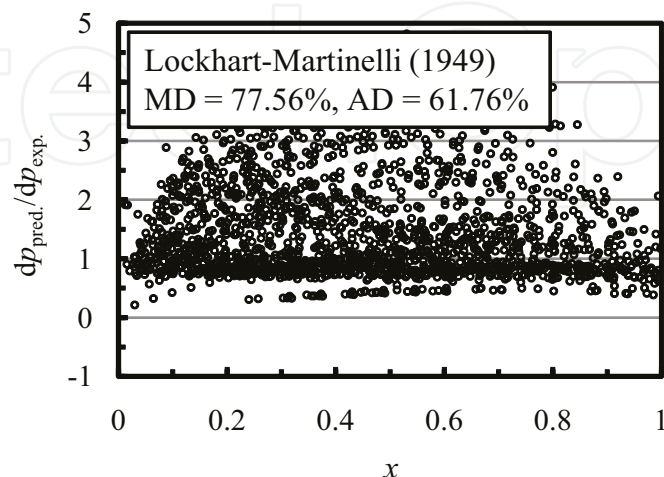

Fig. 9. (j) Comparison between the experimental data and the prediction pressure drop with Lochart-Martinelli (1949) correlation

The pressure drop homogenous model of Beattie and Whalley (1982) provided the best prediction in the A.S. Pamitran et al. (2010) study among the other methods, yielding a mean deviation of around 23%. Mishima and Hibiki (1996) is the best correlation to predict the pressure drop in K.-I Choi et al. (2009) with a mean deviation about 35%. The other presented homogenous models also provided relatively good predictions. The homogenous model assumes that vapor and liquid velocities are equal. The McAdams et al. (1954) correlation was developed based on a homogeneous model. The homogeneous model is a simplification model; therefore, the model is not an empirical model. For some conditions, the homogeneous model can predict the pressure drop well, but not for other conditions; it depends on how close the conditions are to the assumptions of the homogenous model. In this study we develop a new correlation based on the present experimental data. The prediction by the Chang et al.'s (2000) and Friedel's (1979) models yielded a deviation of lower than 28% in every study. The Chang et al. (2000) model was developed with R-410A and air–water in a 5 mm smooth tube. Friedel's (1979) model was developed using a large database; it was valid for horizontal flow and vertical upward flow. The prediction with the Chisholm (1983) method showed a fair result with a mean deviation of lower than 40%. The remaining predictions of Tran et al. (2000), Zhang and Webb (2001), Lockhart and Martinelli (1949) provided a large mean deviation of more than 40% in every study as mentioned in Table 4. The correlations have failed to predict the experimental data of A.S Pamitran et al. (2010) and (2007) and K.-I. Choi et al. (2009) and (2008). Table 5 shows the previous correlations as comparisons, predicting the pressure drop by using the experimental data.

Previous Correlations	
Homogeneous [Beattie and Whalley (1982)]	$\bar{\mu} = \mu_f \left(1 - \dfrac{x\rho_f}{x\rho_f + (1-x)\rho_g} \right) \left(1 - \dfrac{2.5x\rho_f}{x\rho_f + (1-x)\rho_g} \right) + \mu_g \dfrac{x\rho_f}{x\rho_f + (1-x)\rho_g}$
Homogeneous [Cicchitti et al (1960)]	$\bar{\mu} = x\rho_g + (1-x)\rho_f$
Homogeneous [McAdams (1954)]	$\bar{\mu} = \left(\dfrac{x}{\mu_g} \dfrac{1-x}{\mu_f} \right)^{-1}$
Chang et al. (2000)	$\phi_{fo}^2 = (1-x)^2 + x^2 \left[(\rho_f f_{go})/(\rho_g f_{fo}) \right] + 3.24 A_2 A_3 Fr^{-0.045} We^{-0.035+\Phi}$ $A_2 = x^{0.78}(1-x)^{0.224}$, $A_3 = (\rho_f/\rho_g)^{0.91} (\mu_g/\mu_f)^{0.19} [1 - (\mu_g/\mu_f)]^{0.7}$ $\Phi = e^{-\left(\frac{D_{i,ref}}{D_i}\right)^{1.7}} \log\left(\dfrac{350}{We\left(\frac{Re_{fo}}{Re_{fo,ref}}\right)^{1.3}} \right)$
Homogeneous [Dukler et al. (1964)]	$\bar{\mu} = \mu_f \left(1 - \dfrac{x\rho_f}{x\rho_f + (1-x)\rho_g} \right) + \mu_g \dfrac{x\rho_f}{x\rho_f + (1-x)\rho_g}$

Previous Correlations	
Friedel (1979)	$\phi_{\text{fo}}^2 = (1-x)^2 + x^2\left[\left(\rho_f f_{\text{go}}\right)/\left(\rho_g f_{\text{fo}}\right)\right] + 3.24 A_2 A_3 \text{Fr}^{-0.045}\text{We}^{-0.035}$ $A_2 = x^{0.78}(1-x)^{0.224}$, $A_3 = \left(\rho_f/\rho_g\right)^{0.91}\left(\mu_g/\mu_f\right)^{0.19}\left[1-\left(\mu_g/\mu_f\right)\right]^{0.7}$
Chisholm (1983)	$\phi_{\text{fo}}^2 = 1 + \left(\Gamma^2 - 1\right)\left[Bx^{0.875}(1-x)^{0.875} + x^{1.750}\right],$ where $\Gamma^2 = \dfrac{(dp/dz)_{\text{go}}}{(dp/dz)_{\text{fo}}}$ <table><tr><td>Γ</td><td>G (kg m^{-2} s^{-1})</td><td>B</td></tr><tr><td rowspan="3">≤ 9.5</td><td>≤ 500</td><td>4.8</td></tr><tr><td>$500 < G < 1900$</td><td>$2400/G$</td></tr><tr><td>≥ 1900</td><td>$55/G^{0.5}$</td></tr><tr><td rowspan="2">$9.5 < \Gamma < 28$</td><td>≤ 600</td><td>$520/(\Gamma G^{0.5})$</td></tr><tr><td>> 600</td><td>$21/\Gamma$</td></tr><tr><td>≥ 28</td><td>-</td><td>$\Gamma^2 G^{0.5}$</td></tr></table>
Tran et al. (2000)	$\phi_{\text{fo}}^2 = 1(4.3\Gamma^2 - 1)\left[N_{\text{conf}}x^{0.875} + x^{1.75}\right]$ $\Gamma^2 = \dfrac{(dp/dz)_{\text{go}}}{(dp/dz)_{\text{fo}}}$ and $N_{\text{conf}} = \dfrac{\left[\alpha/\left(g(\rho_f - \rho_g)\right)\right]^{0.5}}{D}$
Zhang and Webb (2001)	$\phi_{\text{fo}}^2 = (1-x)^2 + 2.87x^2\left(\dfrac{P}{P_c}\right)^{-1} + 1.68x^{0.8}(1-x)^{0.25}\left(\dfrac{P}{P_c}\right)^{-1.64}$
Mishima and Hibiki (1996)	$\phi_f^2 = 1 - \dfrac{C}{X} + \dfrac{1}{X^2}$ where $X = \left(-\dfrac{dp}{dz}F\right)_f \Big/ \left(-\dfrac{dp}{dz}F\right)_g$ and $C = 21\left(1 - e^{-319\times10^{-6}}\right)$
Lockhart and Martinelli (1949)	$\phi_f^2 = 1 - \dfrac{C}{X_{\text{tt}}} + \dfrac{1}{X_{\text{tt}}^2}$ $X_{\text{tt}} = \left(\dfrac{1-x}{x}\right)^{0.9}\left(\dfrac{\rho_g}{\rho_f}\right)^{0.5}\left(\dfrac{\mu_f}{\mu_g}\right)^{0.1}$ and C(turbulent − turbulent) $= 20$

Table 5. Some of previous correlations to predict pressure drop used by S. Pamitran et al. (2010) and (2007) and K.-I. Choi et al. (2009) and (2008)

4.3 Heat transfer coefficient

Fig. 10(a) shows the effect of mass flux on heat transfer coefficient. Mass flux has an insignificant effect on the heat transfer coefficient in the low quality region. The insignificant

effect of mass flux on the heat transfer coefficient indicates that nucleate boiling heat transfer is predominant. Several previous studies performed by Kew and Cornwell (1997), Lazarek and Black (1982), Wambsganss et al. (1993), Tran et al. (1996) and Bao et al. (2000) used small tubes and showed that, in small channels, nucleate boiling tends to be predominant. The high amount of nucleate boiling heat transfer occurs because of the physical properties of the refrigerants, namely their surface tension and pressure, and the geometric effect of small channels. A higher mass flux corresponds to a higher heat transfer coefficient at moderate-high vapor quality, due to an increase in the convective boiling heat transfer contribution.
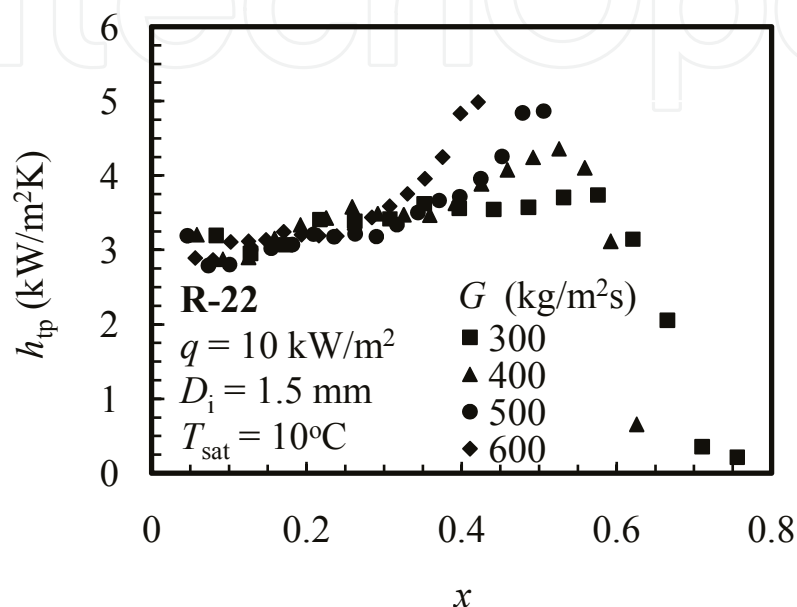
Fig. 10. (a) Effect of mass flux on heat transfer coefficient for R-22 at $q = 10 \text{ kW/m}^2$, $D_i = 1.5$ mm, $T_{sat} = 10°C$
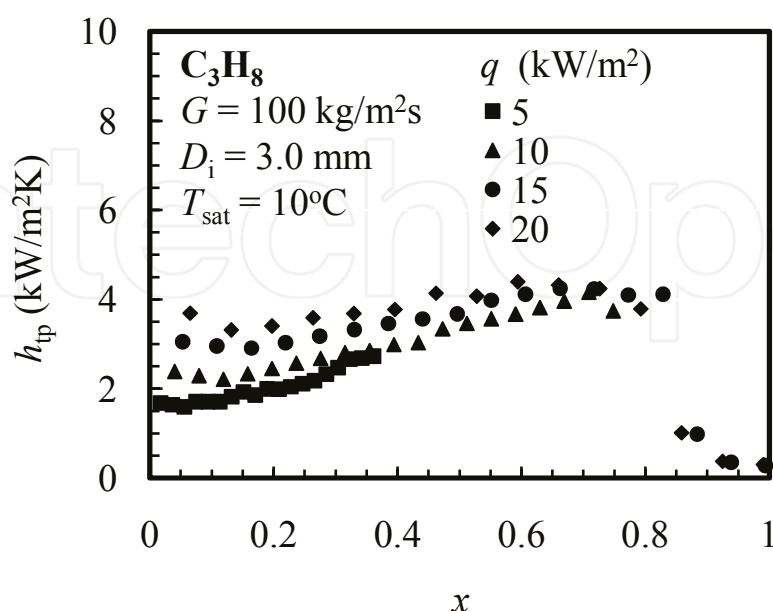
Fig. 10. (b) Effect of heat flux on heat transfer coefficient for C_3H_8 at $G = 100 \text{ kg/}/(\text{m}^2 \cdot \text{s})$, $D_i = 3.0$ mm, $T_{sat} = 10°C$
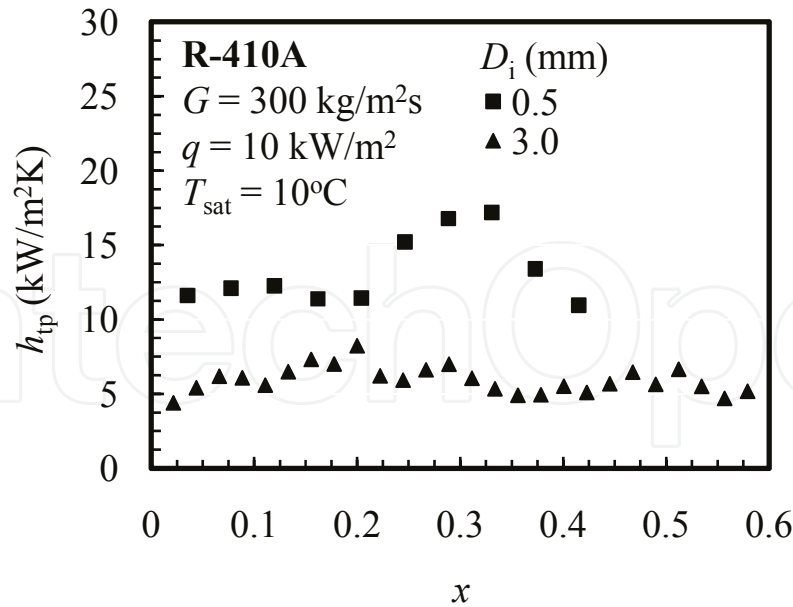
Fig. 10. (c) Effect of inner tube diameter on heat transfer coefficient for R-410A at
G = 300 kg//(m² ·s), q = 10 kW/m², T_{sat} = 10°C
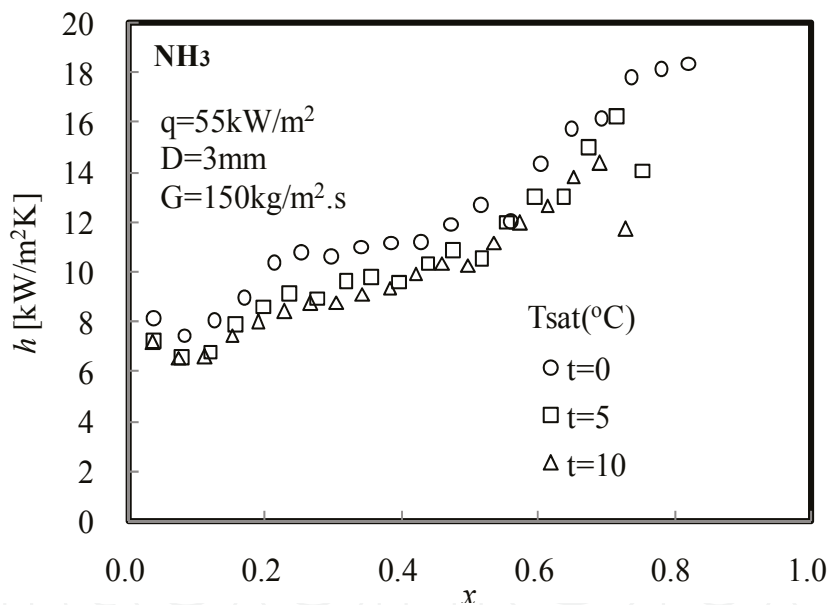
Fig. 10. (d) Effect of saturation temperature on heat transfer coefficient for NH_3 at
G = 150 kg//(m² ·s), q = 55 kW/m², D_i = 3.0 mm

In the high quality region, a drop in the heat transfer coefficient occurs at lower qualities for a relatively higher mass flux. The steep decreasing of the heat transfer coefficient at high qualities is due to the effect of a small diameter tube on the boiling flow pattern because dry-patch occurs more easily in smaller diameter tubes and at a higher mass flux.

Fig. 10(b). depicts the dependence of heat flux on heat transfer coefficients in the low-moderate quality region. The large effect of heat flux on the heat transfer coefficient shows the domination of the nucleate boiling heat transfer contribution. At the higher quality region nucleate boiling is suppressed or convective heat transfer contribution is predominant; this is indicated by a low effect of heat flux on heat transfer coefficient.

Fig. 10 (c) shows that a smaller inner tube diameter has a higher heat transfer coefficient at low quality regions. This is due to a more active nucleate boiling in a smaller diameter tube. As the tube diameter gets smaller, the contact surface area for heat transfer increases. The more active nucleate boiling causes dry-patches to appear earlier. The quality for a rapid decrease in the heat transfer coefficient is lower for the smaller tube. It is supposed that the annular flow appears at a lower quality in the smaller tube and therefore, the dry-out quality is relatively lower for the smaller tube. The effect of saturation temperature on heat transfer coefficient is depicted in Fig. 10 (d). The heat transfer coefficient increases with an increase in saturation temperature, which is due to a larger effect from nucleate boiling. A higher saturation temperature provides a lower surface tension and higher pressure. The vapor formation in the boiling process explains that a lower surface tension and higher pressure provides a higher heat transfer coefficient.

	Previous Correlation	Deviation	
		Mean (%)	Average (%)
K.-I. Choi et al. (2009)	Shah (1988)	19.21	3.55
	Tran et al. (1996)	21.18	-6.15
	Jung at al. (1989)	26.05	23.38
	Gungor and Winterton (1987)	28.44	23.78
	Takamatsu et al (1993)	32.69	32.15
	Kandlikar and Stainke (2003)	33.84	24.41
	Wattelet et al (1994)	48.28	48.28
	Chen (1966)	50.82	18.74
	Zhang et al. (2004)	79.21	77.89
K.-I. Choi et al. (2007)	Wattelet et al.	0.06	-3.03
	Gungore-Winterton	17.48	1.59
	Zhang et al	19.83	-13.35
	Kandlikare-Steinke	21.12	-15.43
	Tran et al.	22.31	-17.37
	Jung et al.	29.1	-23.44
K.-I. Choi et al. (2007)	Wattelet et al.	19.09	12.22
	Jung et al.	23.48	9.53
	Kandlikare-Steinke	24.32	13.05
	Tran et al.	24.81	-10.51
	Shah	25.22	-12.29
	Gungore-Winterton	25.26	2.39
	Chen	36.13	-18.48
A.S. Pamitran et al (2007)	Zhang et al	27.45	-17.34
	Gungore-Winterton	31.07	-12.65
	Tran et al.	31.69	-28.52
	Takamatsu et al.	33.22	-20.65
	Jung et al.	33.39	-26.45
	Kandlikare-Steinke	38.59	-18.39
	Wattelet et al.	38.68	-31.48

Table 6. Mean deviation and average deviation calculated for the different pressure drop prediction methods

Fig. 11 (a) and 11 (b) show the comparisons of the heat transfer coefficients of R-22, R-134a, R-410A, C_3H_8 and CO_2 at some experimental conditions. The mean heat transfer coefficient ratio of R-22, R-134a, R-410A, C_3H_8 and CO_2 was approximately 1.0 : 0.8 : 1.8 : 0.7 : 2.0.
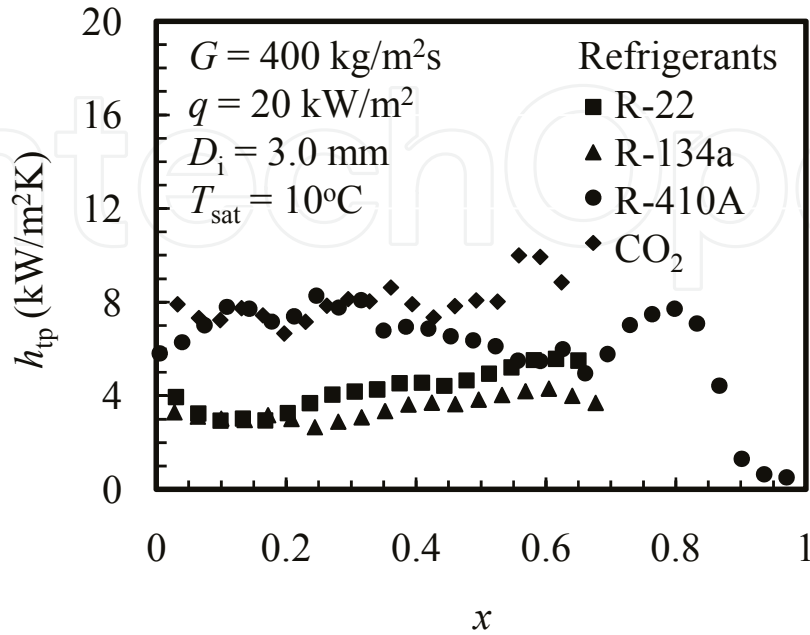
Fig. 11. (a) Heat transfer coefficient comparison of the present working refrigerants at $G = 400$ kg//(m² ·s), $q = 20$ kW/m², $D_i = 3.0$ mm, $T_{sat} = 10$ °C
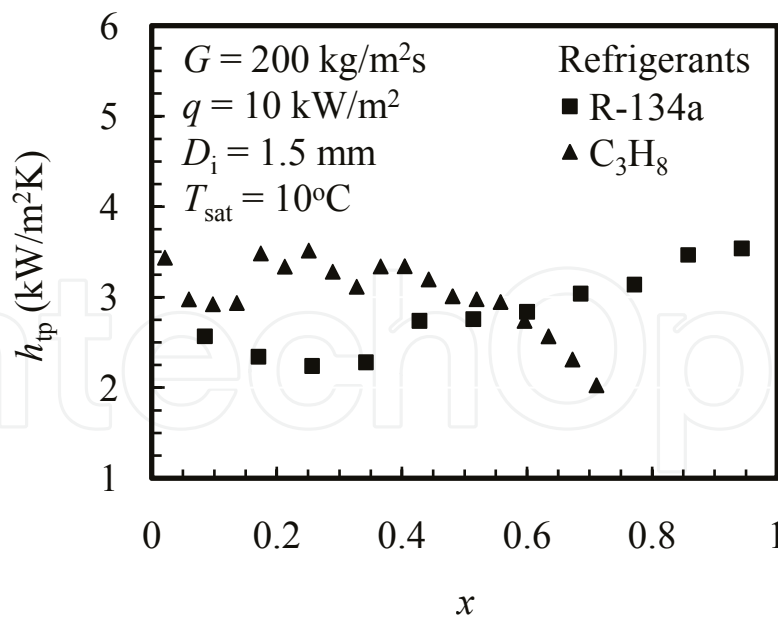
Fig. 11. (b) Heat transfer coefficient comparison of the present working refrigerants at $G = 200$ kg//(m² ·s), $q = 10$ kW/m², $D_i = 1.5$ mm, $T_{sat} = 10$°C

The heat transfer coefficient of CO_2 was higher than that of the other working refrigerants during evaporation under all test conditions. The higher heat transfer coefficient of CO_2 is believed to be due to its high boiling nucleation. The CO_2 has much lower surface tension

and applies much higher pressure than the other working refrigerants. The heat transfer coefficients of R-22, R-134a and C_3H_8 are similar due to their similar physical properties. The comparisons of the physical properties of the present working refrigerants are given in Table 3. The CO_2 has a much lower viscosity ratio μ_f/μ_g than the other working refrigerants, which means that the liquid film of CO_2 can break more easily than those of the other refrigerants. The CO_2 has also a much lower density ratio ρ_f/ρ_g than the other working refrigerants, which leads to a lower vapor velocity, which in turn causes less suppression of nucleate boiling, as shown.

The heat transfer coefficients of the present study are compared with the results given by several correlations for boiling heat transfer coefficients as shown in Table 6. The Gungor-Winterton (1987), Jung et al. (1989), Shah (1988) and Tran et al. (1996) correlations provided better predictions, with mean deviations of lower than 30% in A.S. Pamitran et al (2010), than the other correlations. Wattelet et al (1994) successively predict the experiment data for [a,b]K.I. Choi et al (2007). The Gungor-Winterton (1987) correlation was a modification of the superposition model; it was developed using fluids in several small and conventional tubes under various test conditions. The Jung et al. (1989) correlation was developed with pure and mixture refrigerants in conventional channels; its *F* factor contributed a big calculation deviation with the current experimental data. The Shah (1988) correlation was developed using a large data set for conventional tubes. The prediction with the Shah (1988) correlation was fair under conditions at the low quality region. The Tran et al. (1996) correlation was developed for R-12 and R-113 in small tubes. The correlations of Chen (1966) and Wattelet et al. (1994), which were developed for large tubes, have a high prediction deviation in K.I Choi et al.'s (2009) experimental data. The correlations of Kandlikar (1990) and Zhang et al. (2004) were developed for small tubes; however, the correlations could not predict well the present experimental data. The correlations of Wattelet et al. (1994), Kandlikar (1990) and Zhang et al. (2004) showed a large deviation in the prediction of the CO_2 data. The Kandlikar (1990) correlation failed to predict the heat transfer coefficient at the high quality region.

Table 7 shows the previous correlation use by A.S. Pamitran et al. (2007) and K.I Choi (2009), (2007)

5. Development of a new correlation

5.1 Pressure drop

In this section, the effort of A.S. Pamitran et al and Choi et al. in developing a pressure drop correlation that is appropriate to use in specific refrigerants for the horizontal smooth minichannel is highlighted. The area average-gas fraction or void fraction denoted with α is defined as the ratio of gas phase cross-sectional area (A_g) to the total cross-sectional area. $A = A_g + A_f$

$$\alpha = \frac{A_g}{A} \tag{12}$$

In boiling and condensation it is often convenient to use the fraction of the total mass flow which is composed of vapor or liquid. The mass quality, *x*, is defined as

$$x = \frac{W_g}{W_g + W_f} = \frac{W_g}{W} \tag{13}$$

Heat Transfer Coefficient Correlations	
Gungor and Winterton (1987)	$h_{\text{tp}} = E.h_l + S.h_{\text{pb}}$ $E = \text{fn}(Bo, X_{\text{tt}})$ and $S = \text{fn}(Bo, X_{\text{tt}}, Re_l)$ $h_l = h_{\text{Dittus-Boelter}}$, $h_{\text{pb}} = h_{\text{Cooper}}$
Jung et al. (1989)	$h_{\text{tp}} = \dfrac{N}{C_{\text{un}}} h_{\text{un}} + C_{\text{me}} F_{\text{p}} h_{\text{lo}}$ $N = \text{fn}(X_{\text{tt}}, Bo)$ $C_{\text{un}} = \text{fn}(X, Y, p, p_{cmvc})$ $h_{\text{un}} = \dfrac{h_1 h_2}{(h_1 X_2 + h_2 X_1)}$, h_1 and h_2 are $h_{sa} = h_{Stephan-Abdesalam}$ $C_{\text{me}} = \text{fn}(X, Y)$, $F_{\text{p}} = \text{fn}(X_{\text{tt}})$ $h_{\text{lo}} = h_{\text{Dittus-Boelter}}$
Shah (1988)	For horizontal tube, $Fr_f > 0.04$ $N = C_o = \left(\dfrac{1-x}{x}\right)^{0.8} \left(\dfrac{\rho_g}{\rho_f}\right)^{0.5}$ $h_{\text{tp}} = max(h_{\text{nb}}, h_c)$
Tran et al. (1996)	$h_{\text{tp}} = 8.4 \times 10^2 (Bo^2 We_f)^{0.3} \left(\dfrac{\rho_f}{\rho_g}\right)^{-0.4}$
Chen (1966)	$h_{\text{tp}} = S.h_{\text{nb}} + F.h_{lo}$ $h_{\text{nb}} = h_{\text{Foster-Zuber}}$ $h_{\text{lo}} = h_{\text{Dittus-Boelter}}$ $F = \text{fn}(X_{\text{tt}})$ and $S = \text{fn}(Re_{\text{tp}})$
Wattelet et al.(1994)	$h_{\text{tp}} = [h_{\text{nb}}^n + h_{\text{cb}}^n]^{1/2}$, $n = 2.5$ $h_{\text{nb}} = h_{\text{Cooper}}$ $h_{\text{cb}} = h_{\text{Dittus-Boelter}} \times F \times R$ $R = \text{fn}(X_{\text{tt}})$ and $R = \text{fn}(Fr_1)$
Kandlikar and Steinke (2003)	$\dfrac{h_{\text{tp}}}{h_l} = D_1 Co^{D_2}(1-x)^{0.8}\text{fn}(Fr_{lo})$ $\qquad\qquad\qquad\qquad + D_3 Bo^{D_4}(1-x)^{0.8}Fn$ $\text{fn}(Fr_{lo}) = 1$
Zang et al. (2004)	$h_{\text{tp}} = S.h_{\text{nb}} + F.h_{\text{sp}}$ for horizontal circular channel $h_{\text{nb}} = h_{\text{Foster-Zuber}}$ $h_{\text{sp}} = max(h_{\text{Dittus-Boelter}})$, if $Re_f < 2300$ $h_{\text{sp}} = h_{\text{Dittus-Boelter}}$, if $Re_f \geq 2300$ $F = \text{fn}(\phi_f)$ and $S = \text{fn}(Re_f)$

Table 7. Some of previous correlations to predict heat transfer coefficient used by .S Pamitran et al. (2010) and (2007) and K.-I. Choi et al. (2009) and (2008)

The rate of mass flow divided by the flow area is given in the name 'mass velocity' and the symbol G.

$$G = \frac{W}{A} = \rho.u = \frac{u}{v} \tag{14}$$

The mean velocity of the liquid phase is shown by

$$u_f = \frac{G(1-x)}{\rho_f.(1-\alpha)} \tag{15}$$

The mean velocity of the gas phase is shown by

$$u_g = \frac{Gx}{\rho_g.\alpha} \tag{16}$$

The total pressure drop consists of friction, acceleration and static head components as illustrated in the Equation below.

$$\left(\frac{dp}{dz}\right) = \left(\frac{dp}{dz}F\right) + \left(\frac{dp}{dz}a\right) + \left(\frac{dp}{dz}z\right)$$

For flow boiling in a horizontal layout test section, the static head pressure drop is excluded. Therefore, the experimental two-phase frictional pressure drop can be obtained by subtracting the calculated acceleration pressure drop from the measured pressure drop, as shown in Eq. (2), and may then be expressed in terms of the single-phase pressure drop for the liquid phase, considered to exist in the tube, as below.

$$\left(\frac{dp}{dz}F\right) = \left(\frac{dp}{dz}F\right)_f \phi_f^2 \tag{17}$$

The liquid frictional pressure drop is calculated from the Fanning equation. The frictional pressure drop can then be rewritten as Eq. (19) below.

$$\left(\frac{dp}{dz}F\right)_f = \frac{2f_f G^2(1-x)^2}{\rho_f D} \tag{18}$$

The friction factor in Eq. (7) was obtained by considering the flow conditions of laminar–turbulent flows, where $f = 16Re^{-1}$ for Re < 2300 (laminar flow) and $f = 0.079\ Re^{-0.25}$ for Re > 3000 (turbulent flow). The laminar–turbulent transition Reynolds number was obtained from Yang and Lin (2007).

$$\left(\frac{dp}{dz}F\right) = \left[\frac{2f_f G^2(1-x)^2}{\rho_f D}\right] \phi_f^2 \tag{19}$$

A new modified pressure drop correlation was developed on the basis of the Lockhart–Martinelli method. The two-phase pressure drop of Lockhart–Martinelli consists of the following three terms: the liquid phase pressure drop, the interaction between the liquid phase and the vapor phase, and the vapor phase pressure drop. The relationship among these terms is expressed in Eq. (20).

$$\left(-\frac{dp}{dz}F\right)_{tp} = \left(-\frac{dp}{dz}F\right)_f + C\left[\left(-\frac{dp}{dz}F\right)_f\left(-\frac{dp}{dz}F\right)_g\right]^{1/2} + \left(-\frac{dp}{dz}F\right)_g \qquad (20)$$

The two-phase frictional multiplier based on the pressure gradient for liquid alone flow, ϕ_f^2, is calculated by dividing Eq. (20) by the liquid phase pressure drop, as is shown in Eq. (21).

$$\phi_f^2 = \frac{\left(-\frac{dp}{dz}F\right)_{tp}}{\left(-\frac{dp}{dz}F\right)_f} = 1 + C\left[\frac{\left(-\frac{dp}{dz}F\right)_g}{\left(-\frac{dp}{dz}F\right)_f}\right]^{1/2} + \frac{\left(-\frac{dp}{dz}F\right)_g}{\left(-\frac{dp}{dz}F\right)_f} = 1 + \frac{C}{X} + \frac{1}{X^2} \qquad (21)$$

The Martinelli parameter, X, is defined by the following equation:

$$X = \left[\frac{\left(-\frac{dp}{dz}F\right)_f}{\left(-\frac{dp}{dz}F\right)_g}\right]^{1/2} = \left[\frac{2f_f G^2(1-x)^2\rho_g/D}{2f_g G^2 x^2\rho_f/D}\right]^{1/2} = \left(\frac{f_f}{f_g}\right)^{1/2}\left(\frac{1-x}{x}\right)\left(\frac{\rho_g}{\rho_f}\right)^{1/2} \qquad (22)$$

The friction factor in Eq. (22) was obtained by considering the flow conditions of laminar (for Re < 1000, $f = 16\text{Re}^{-1}$) and turbulent (for Re > 2000, $f = 0.079\text{Re}^{-0.25}$).
The pressure drop prediction method can be summarized as follows:

$$\left(\frac{dp}{dz}\right) = \left(\frac{dp}{dz}F\right) + \left(\frac{dp}{dz}a\right)$$

$$\left(\frac{dp}{dz}\right) = \left(\frac{2f_f G^2(1-x)^2}{\rho_f D}\right)\phi_f^2 + G^2\frac{d}{dz}\left(\frac{x^2}{\alpha\rho_g} + \frac{(1-x)^2}{(1-\alpha)\rho_f}\right)$$

$$\left(\frac{dp}{dz}\right) = \left(\frac{2f_f G^2(1-x)^2}{\rho_f D}\right)\left(1 + \frac{C}{X} + \frac{1}{X^2}\right) + G^2\frac{d}{dz}\left(\frac{x^2}{\alpha\rho_g} + \frac{(1-x)^2}{(1-\alpha)\rho_f}\right)$$

$$\left(\frac{dp}{dz}\right) = \left(\frac{2f_f G^2(1-x)^2}{\rho_f D}\right)\left(1 + \frac{C}{\left(\frac{f_f}{f_g}\right)^{1/2}\left(\frac{1-x}{x}\right)\left(\frac{\rho_g}{\rho_f}\right)^{1/2}} + \frac{1}{\left(\frac{f_f}{f_g}\right)\left(\frac{1-x}{x}\right)^2\left(\frac{\rho_g}{\rho_f}\right)}\right)$$
$$+ G^2\frac{d}{dz}\left(\frac{x^2}{\alpha\rho_g} + \frac{(1-x)^2}{(1-\alpha)\rho_f}\right) \qquad (23)$$

The calculated factor C is obtained from Chisholm (1967). For the liquid-vapor flow condition of turbulent-turbulent (tt), laminar-turbulent (vt), turbulent-laminar (tv) and laminar-laminar (vv), the values of the Chisholm (1967) parameter, C, are 20, 12, 10, and 5, respectively. The value of C in this thesis is obtained by considering the flow conditions of laminar and turbulent with thresholds of Re=2300 and Re=3000 for the laminar and turbulent flows, respectively. The laminar-turbulent transition Reynolds number was obtained from Yang and Lin (2007). Fig. 12 shows a comparison of the two-phase frictional multiplier data with the values predicted by the Lockhart-Martinelli correlation with C=5 and C=20. The figure shows that the present data are located at mostly between the baseline of C=5 and C=20, which means that laminar, turbulent and the co-current laminar-turbulent flows exist in the present data. For liquid-vapor flow conditions, the present experimental

data shows 5.43% laminar-laminar, 28.46% laminar-turbulent, 3.78% turbulent-laminar, and 62.33% turbulent-turbulent.
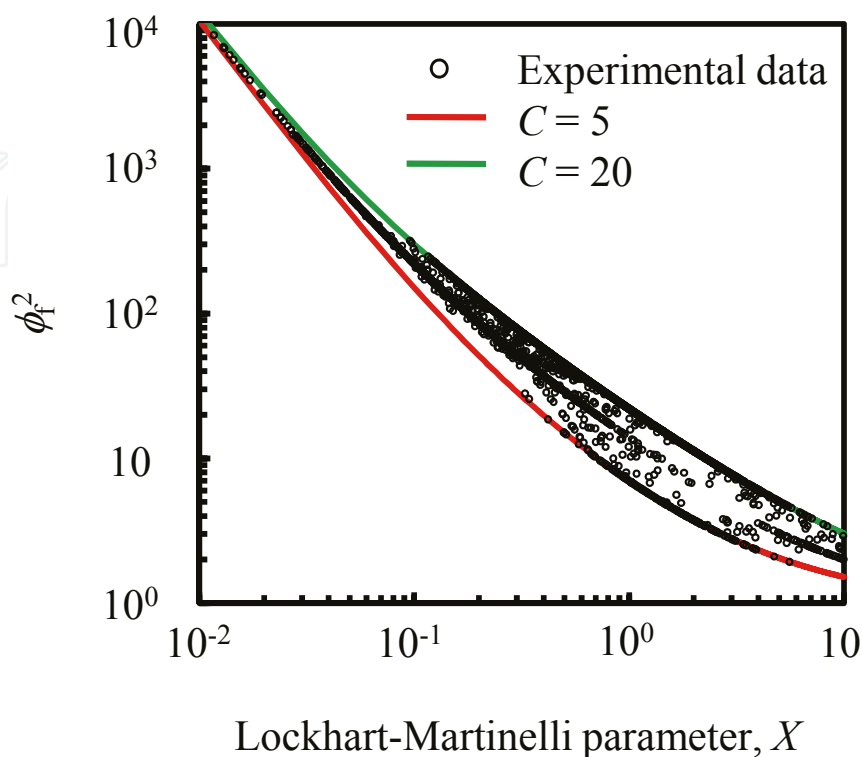
Fig. 12. Variation of the two-phase frictional multiplier data with the Lockhart-Martinelli parameter

The experimental result showed that the pressure drop is a function of mass flux, inner tube diameter, surface tension, density and viscosity, therefore the factor C in Eq. (21) and (23) will be developed as a function of the two-phase Weber number, We_{tp}, and the two-phase Reynolds number, Re_{tp}.

$$C = \left(\phi_f^2 - 1 - \frac{1}{X^2} \right) X = fn(We_{tp}, Re_{tp}) \tag{24}$$

Where We_{tp} and Re_{tp} are defined as:

$$We_{tp} = \frac{G^2 D}{\bar{\rho}\sigma} \tag{25}$$

$$Re_{tp} = \frac{GD}{\bar{\mu}} \tag{26}$$

A new factor C was developed using the regression method, as is shown in the Equations in the table below.

A new pressure drop correlation was developed on the basis of the Lockhart–Martinelli method as a function of the Weber number, We_{tp}, and the Reynolds number, Re_{tp} by considering the laminar–turbulent flow conditions. Using a regression method with 812 data

points, a new factor C was developed by A.S. Pamitran et al. (2010) with mean and average deviations of 21.66% and -2.47%, respectively, based on comparison as shown in Fig. 13.

	Correlation	Deviation
Pamitran, A.S., et al. (2010)	$C = 3 \times 10^{-3} \times Re_{tp}^{1.23} We_{tp}^{-0.433}$	MD = 21.66% AD = -2.47%
Choi, K.-I., et al. (2009)	$C = 1732.953 \times Re_{tp}^{-0.323} We_{tp}^{-0.24}$	MD = 10.84% AD = 1.08%
Choi, K.-I., et al. (2008)	$C = 5.5564 \times Re_{tp}^{0.2837} We_{tp}^{-0.288}$	MD = 4.02 AD = -0.14%
Pamitran, A.S., et al. (2008)	$C = 1.2897 \times 10^6 \times Re_{tp}^{0.5674} We_{tp}^{-3.3271}$	MD = 9.41% AD = -0.55%

Table 8. Equations developed by A.S. Pamitran et al. and K.I. Choi et al

This correlation will contribute to the design of heat exchangers with small tubes.
Fig. 14 illustrates the two-phase frictional multiplier comparison between the present experimental data and the prediction with the newly developed correlation. The comparison shows a mean deviation of 10.84% and an average deviation of 1.08%.
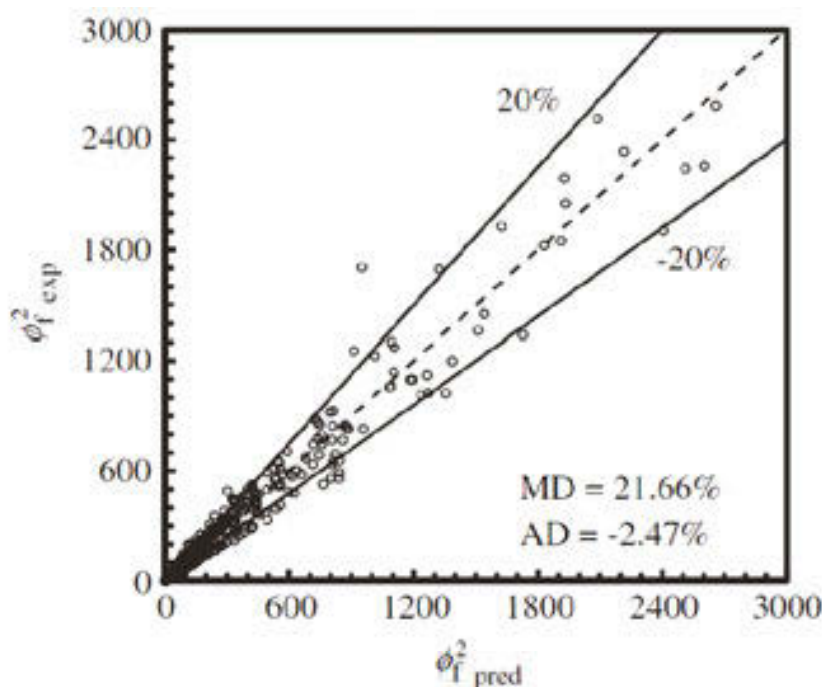

Fig. 13. Two-phase frictional multiplier comparison between the present experimental data ($\phi^2_{f\,exp}$) and the prediction with the newly developed correlation ($\phi^2_{f\,pred}$), A.S. Pamitran et al. (2010)
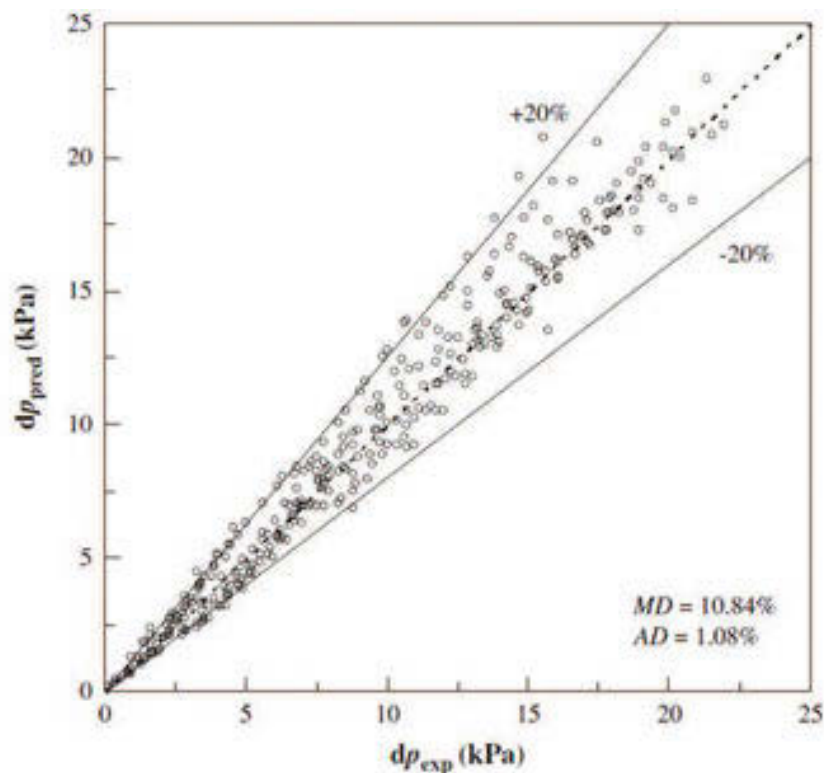
Fig. 14. Comparison of the experimental and predicted heat transfer coefficients using the new developed correlation. K.I. Choi et al (2009)

5.2 Heat transfer coefficient

It is well known that the flow boiling heat transfer is mainly governed by two important mechanisms, namely nucleate boiling and forced convective heat transfer.

$$h_{tp} = h_{nb} + h_c \qquad (27)$$

In two-phase flow boiling heat transfer, the nucleate boiling heat transfer contribution is suppressed by the two-phase flow. Therefore, the nucleate boiling heat transfer contribution may be correlated with a nucleate boiling suppression factor, S. Another contribution of convective heat transfer may be correlated with a liquid single phase heat transfer. The F factor is introduced as a convective two-phase multiplier to account for enhanced convective properties due to co-current flow of liquid and vapor. A superposition model of heat transfer coefficient may be written as follows:

$$h_{tp} = S.h_{nbc} + F.h_f \qquad (28)$$

The appearance of convective heat transfer for boiling in small channels occurs later than it does in large channels because of its high boiling nucleation.

The new heat transfer coefficient correlation in this study is developed by only using the experimental data prior to the dry-out. Chen (1966) introduced a multiplier factor, F= fn(X_{tt}), to account for the increase in the convective turbulence that is due to the presence of the vapor phase. The function should be physically evaluated again for flow boiling heat transfer in a minichannel that has a laminar flow condition, which is due to the small diameter effect. By considering the flow conditions (laminar or turbulent) in the Reynolds

number factor, F, Zhang et al. (2004) introduced a relationship between the factor F and the two-phase frictional multiplier that is based on the pressure gradient for liquid alone flow, ϕ_f^2. This relationship is

$$F = fn(\phi_f^2) \tag{29}$$

Where ϕ_f^2 is a general form for four conditions according to Chisholm (1967), as is shown in Eq. (21). For the liquid–vapor flow condition of turbulent–turbulent (tt), laminar–turbulent (vt), turbulent–laminar (tv) and laminar–laminar (vv), the values of the Chisholm parameter, C, are 20, 12, 10, and 5, respectively. The value of C is found by an interpolation of the Chisholm parameter with thresholds of Re = 1000 and Re = 2000 for the laminar and turbulent flows, respectively.

The Martinelli parameter is defined as in equation (22) together with the Blasius equation of friction factors, f_f and f_g ; the Martinelli parameter can be rewritten as

$$\left(\frac{f_f}{f_g}\right)^{1/8} \left(\frac{1-x}{x}\right)^{7/8} \left(\frac{\rho_g}{\rho_f}\right)^{1/2} \tag{30}$$

There is an important effect of quality, density ratio, ρ_f/ρ_g, and the viscosity ratio, μ_f/μ_g, on heat transfer coefficient. The liquid heat transfer is defined by existing liquid heat transfer coefficient correlations by considering flow conditions of laminar and turbulent. For laminar flow, $Re_f < 2300$, where

$$Re_f = \frac{G(1-x)D}{\mu_f} \tag{31}$$

And the liquid heat transfer coefficient is obtained from the following correlation:

$$h_f = 4.36 \frac{k_f}{D} \tag{32}$$

For flow with $3000 \leq Re_f \leq 10^4$, the liquid heat transfer coefficient is obtained from the Gnielinski (1976) correlation:

$$h_f = \frac{(Re_f - 1000)Pr_f\left(\frac{f_f}{2}\right)\left(\frac{k_f}{D}\right)}{1 + 12.7\left(Pr_f^{2/3} - 1\right)\left(\frac{f_f}{2}\right)^{0.5}} \tag{33}$$

where the friction factor is calculated from (for Re < 1000, $f = 16Re^{-1}$) and turbulent (for Re > 2000, $f = 0.079Re^{-0.25}$). For flow with $2300 \leq Re_f \leq 3000$, the liquid heat transfer coefficient is calculated by interpolation. For turbulent flow with $10^4 \leq Re_f \leq 5 \times 10^6$, the liquid heat transfer coefficient is obtained from the Petukhov and Popov (1963) correlation:

$$h_f = \frac{Re_f Pr_f\left(\frac{f_f}{2}\right)\left(\frac{k_f}{D}\right)}{1 + 12.7\left(Pr_f^{2/3} - 1\right)\left(\frac{f_f}{2}\right)^{0.5}} \tag{34}$$

The Dittus Boelter (1930) correlation is used for turbulent flow with $Re_f \geq 5 \times 10^6$.

$$h_f = 0.023 \frac{k_f}{D} Re_f^{0.8} Pr_f^{0.4} = 0.23 \frac{k_f}{D} \left[\frac{G(1-x)D}{\mu_f} \right]^{0.8} \left[\frac{Cp_f \mu_f}{k_f} \right]^{0.4} \tag{35}$$

The F factor in this study is developed as a function of ϕ_f^2, $F = \mathrm{fn}(\phi_f^2)$, where ϕ_f^2 is obtained from Eqs. (21) – (22). The liquid heat transfer is defined by the Dittus Boelter correlation and a new factor F, as is shown in Fig. 15(a)-(d), is developed using a regression method.
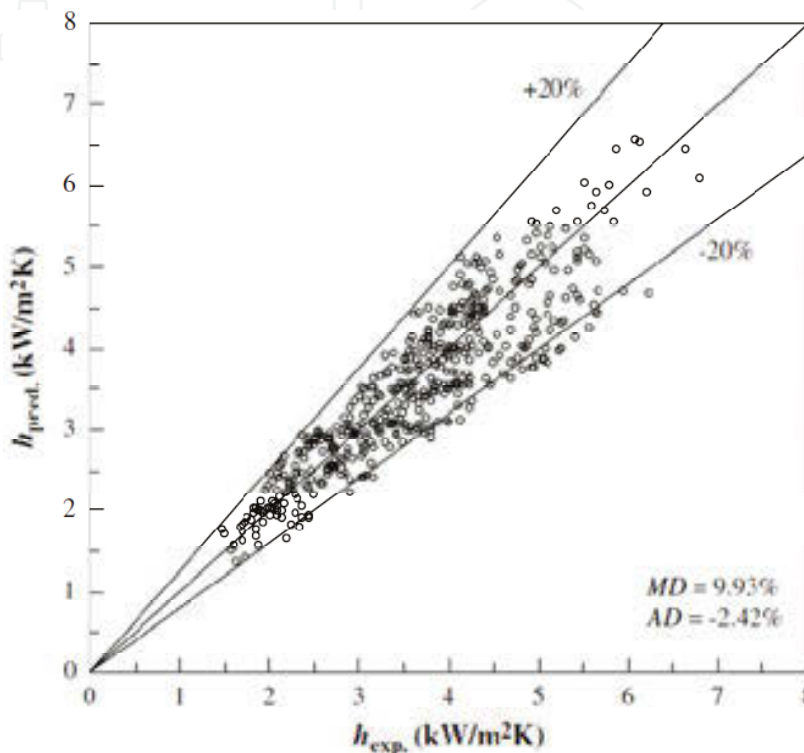
Fig. 15. (a) Comparison of the experimental and predicted heat transfer coefficients using the new developed correlation. K.I. Choi et al. (2009)
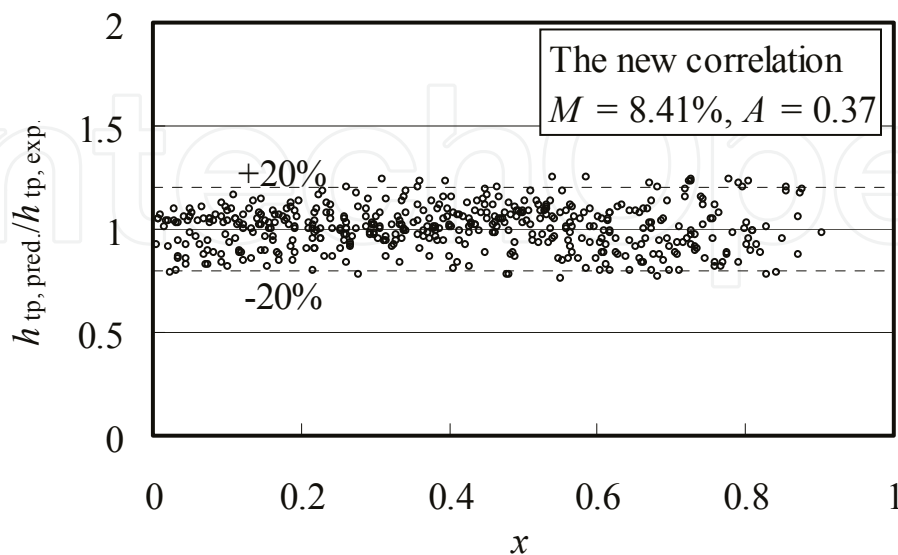
Fig. 15. (b) Diagram of the ratio of the experimental heat transfer coefficient, $h_{tp,exp}$, and the predicted heat transfer coefficient, $h_{tp,pred}$, vs. quality, x. [a]K.I. Choi et al. (2007)
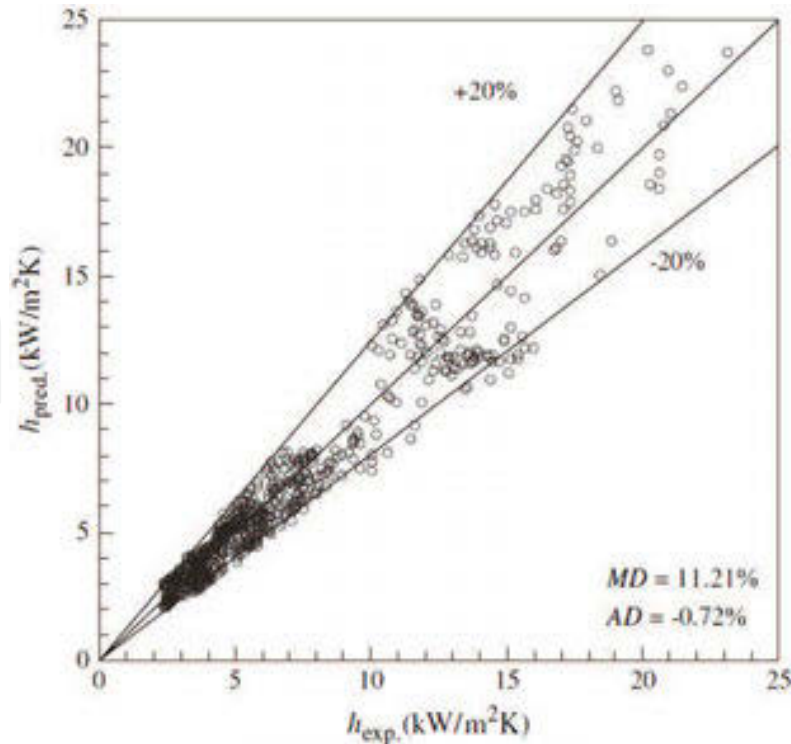
Fig. 15. (c) Diagram of the experimental heat transfer coefficient, $h_{exp.}$, vs prediction heat transfer coefficient, $h_{pred.}$. [b]K.I. Choi et al. (2007)

Fig. 15. (d) Diagram of experimental heat transfer coefficient h_{exp} vs prediction heat transfer coefficient $h_{pred.}$. A.S. Pamitran et al (2007)

The prediction of the nucleate boiling heat transfer for the present experimental data used Cooper (1984), which is a pool boiling correlation developed based on an extensive study.

$$h = 55 p_r^{0.12} (-0.4343 ln p_r)^{-0.55} M^{-0.5} q^{0.67} \qquad (36)$$

Where the heat fluxes, q, is in Wm^{-2}. Kew and Cornwell (1997) and Jung et al. (2003) showed that the Cooper (1984) pool boiling correl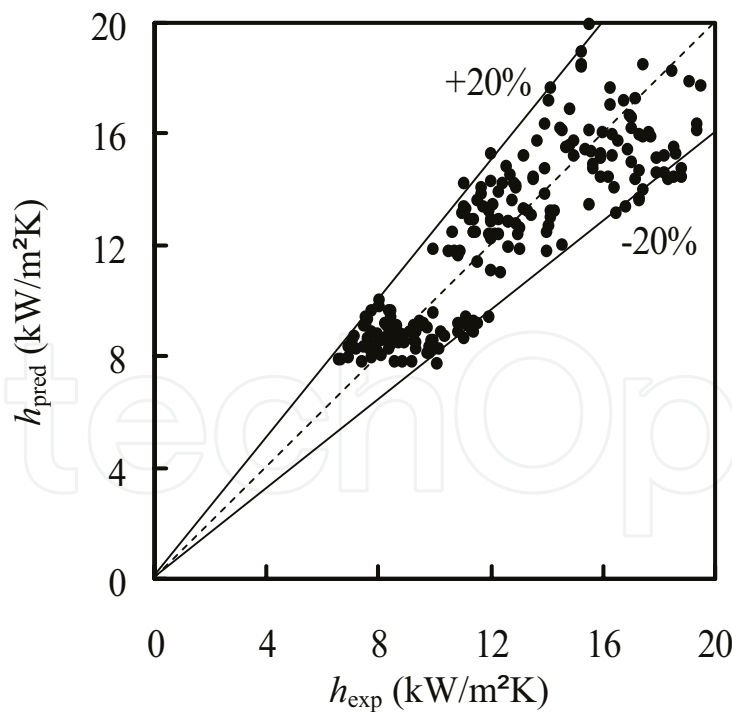ation best predicted their experimental data. Chen (1966) defined the nucleate boiling suppression factor, S, as a ratio of the mean superheat, ΔT_e, to the wall superheat, ΔT_{sat}. Jung et al. (1989) proposed a convective boiling heat transfer multiplier factor, N, as a function of quality, heat flux and mass flow rate (represented by employing Xtt and Bo) to represent the strong effect of nucleate boiling in flow boiling as it is compared with that in nucleate pool boiling, h_{nbc}/h_{nb}. The Martinelli parameter, X_{tt}, is replaced by a two-phase frictional multiplier, ϕ_f^2, in order to consider laminar flow in minichannels. By using the experimental data of this study, a new nucleate boiling suppression factor, as a ratio of h_{nbc}/h_{nb}, is proposed as showen in table 9.

A.S. Pamitran et al. and K.I. Choi et al have developed a correlation based on the Zhang et al (2004) that modified the F factor and Chen (1966) introduced the suppression factor, S. The new heat transfer coefficient correlation is developed using a regression method with 461 data points for C_3H_8 in Choi, K.I et al (2009), 471 data points for CO_2 in [a]K.-I. Choi et al (2007), 681 data points for R-22, R-134a, and R-744 (CO_2) in [b]K.I. Choi et al.(2007), and 217 data points for R-410A in A.S. Pamitran et al. (2007).

The comparison of the experimental heat transfer coefficient, $h_{tp,exp}$, and the predicted heat transfer coefficient, $h_{tp,pred}$, for propane is illustrated in Fig. 15(a). The new correlation agrees closely for the comparison with a mean deviation of 9.93% and an average deviation of -2.42%. Fig. 15(b) illustrates CO_2 on the comparison with a mean deviation of 8.41% and an average deviation of 0.37%.

The comparison of the experimental heat transfer coefficient, h_{exp}, and the prediction heat transfer coefficient, h_{pred}, is shown in Fig. 15(c). The new correlation for three refrigerants R-22, R-134a and R-744 (CO_2) showed good agreement with a mean deviation of 11.21% and an average deviation of -0.72%. Fig 14 (d), the new correlation for 410A also show a suitable range of mean deviation, 11.20% and an average deviation 0.09%; Table 9 gives a summary of the new correlation.

	F factor	Supression factor	Deviation
Choi, K.-I. et al. (2009)	$F = MAX(0.5\phi_f, 1)$	$S = 181.458(\phi_f^2)^{0.002} Bo^{0.816}$	MD = 9.93% AD = 2,42%
[a]K.-I. Choi et al. (2007)	$F = 0.05\phi_f^2 + 0.95$	$S = 7.2694(\phi_f^2)^{0.0094} Bo^{0.2814}$	MD = 8.41% AD = 0.37%
[b]K.-I. Choi et al. (2007)	$F = 0.042\phi_f^2 + 0.958$	$S = 469.1689(\phi_f^2)^{-0.2093} Bo^{0.7402}$	Overall MD = 11.21% AD = -0,72%
A.S. Pamitran et al. (2007)	$F = 0.062\phi_f^2 + 0.938$	$S = 9.4626(\phi_f^2)^{-0.2747} Bo^{0.1285}$	MD= 11.20% AD = 0.09%

Table 9. Equations developed by A.S. Pamitran et al. and K.I. Choi et al

6. Concluding remarks

The pressure drop and heat transfer experiments in convective boiling performed with R-22, R-134a, R-410A, R-744 (CO_2), R-717 (NH_3) and R-290 (C_3H_8) in horizontal smooth

minichannels. It can be explained, that, the pressure drop is higher at the conditions of higher mass and heat fluxes, and for the conditions of smaller inner tube diameter and lower saturation temperature. The experimental results showed that pressure drop is a function of mass flux, inner tube diameter, surface tension, density and viscosity. The new pressure drop correlations were developed on the basis of the Lockhart–Martinelli method as a function of the two-phase Reynolds number, Re_{tp}, and the two-phase Weber number, We_{tp}. The new factor C was developed using a regression method

Mass flux, heat flux, inner tube diameter and saturation temperature have an effect on the heat transfer coefficient. The heat transfer coefficient increases with a decreased inner tube diameter and with an increased saturation temperature. The geometric effect of the small tube must be considered to develop a new heat transfer coefficient correlation.

The two-phase flow pattern was mapped in the Wang et al (1997) and the Wotjan et al.(2005) flow pattern maps. The Wotjan et al. flow pattern map illustrates the formation of intermittent, annular, dry-out, and mist flows until the dry-out. The Wang et al (1997) flow pattern map illustrates the data start from annular flow, Str. wavy to intermittent flow.

Laminar flow appears for flow boiling in small channels, so the modified correlation of the multiplier factor for the convective boiling contribution, F, and the nucleate boiling suppression factor, S, is developed in the study using laminar and turbulent flows consideration. The new boiling heat transfer coefficient correlations that are based on a superposition model for refrigerants in minichannels were presented. The work of developing the new correlations used 2288 data points.

The documentation contained in this manuscript endeavors to perceive the two-phase flow boiling heat transfer and pressure drop in horizontal circular channels as the basic understanding for application in refrigeration fields or any concern that is related to two-phase flow. It is known that there is no single correlation that has the ability to predict accurately the two-phase flow heat transfer and pressure drop. Every single or mixed refrigerant could be had differently as a result of pressure drop correlation and heat transfer correlation. Therefore, the modification of the previous correlations or a new development in this matter is still open.

7. Nomenclature

A   Cross section area

AD   Average Deviation, $\mathrm{AD} = \left(\dfrac{1}{n}\right)\sum\limits_{1}^{n}\left(\left(\mathrm{d}p_{\mathrm{pred}} - \mathrm{d}p_{\mathrm{exp}}\right)\times 100\Big/\mathrm{d}p_{\mathrm{exp}}\right)$ *for pressure drop or*

         $\mathrm{AD} = \left(\dfrac{1}{n}\right)\sum\limits_{1}^{n}\left(\left(h_{\mathrm{pred}} - h_{\mathrm{exp}}\right)\times 100\Big/h_{\mathrm{exp}}\right)$ *for heat transfer coefficient*

Bo   Boiling number, $Bo = q\big/Gi_{\mathrm{fg}}$

C Correction factor for two-phase pressure drop

c_{p} Specific heat capacity at constant pressure (kJ/(kg·K))

D Diameter (m)

E Electric potential (V)

F Multiplier factor for convective heat transfer contribution

f Friction factor

G Mass flux (kg/(m² s))

g Acceleration due to gravity (m/s²)

h Heat transfer coefficient (kW/(m²·K))

I   Electric current (A)
i   Enthalpy (kJ/(kg·K))
k   Thermal conductivity (kW/(m·K))
L   Tube length (m)
M   Molecular weight of the liquid

MD   Mean Deviation, $\mathrm{MD} = \left(\dfrac{1}{n}\right)\sum_1^n \left\| \left(\left(\mathrm{d}p_{\mathrm{pred}} - \mathrm{d}p_{\mathrm{exp}}\right) \times 100 \middle/ \mathrm{d}p_{\mathrm{exp}}\right)\right\|$ *for pressure drop or*

$\mathrm{MD} = \left(\dfrac{1}{n}\right)\sum_1^n \left\| \left(\left(h_{\mathrm{pred}} - h_{\mathrm{exp}}\right) \times 100 \middle/ h_{\mathrm{exp}}\right)\right\|$ *for heat transfer coefficient*

n   Number of data
P   Pressure (N/m²)
Pr   Prandtl number, $\mathrm{Pr} = c_{\mathrm{p}}\mu/k$
Q   Electric power (kW)
q   Heat flux (kW/m²)
q̇   Heat generation (kW/m³)
R   Electrical resistance (ohm)
Re   Reynolds number, $\mathrm{Re} = GD/\mu$
*R*ₚ   Surface roughness parameter (μm)
S   Suppression factor
T   Temperature (K)
V   Volume (m³)
W   Mass flow rate (kg/s)
We   Webber number,
X   Lockhart-Martinelli parameter
x   Mass quality
z   Length (m)

Greek letters

λ   Correction factor on Baker (1954) flow pattern map, $\lambda = \left[\left(\rho_{\mathrm{g}}/\rho_{\mathrm{A}}\right)\left(\rho_{\mathrm{f}}/\rho_{\mathrm{W}}\right)\right]^{1/2}$
a   Void fraction
μ   Viscosity (Pa·s)
ρ   Density (kg/m³)
σ   Surface tension (N/m)
ϕ²   Two-phase frictional multiplier
ψ   Correction factor on Wang et al.(1997) flow pattern map, $\psi = \left(\sigma_{\mathrm{W}}/\sigma\right)^{1/4}\left[\left(\mu_{\mathrm{f}}/\mu_{\mathrm{W}}\right)\left(\rho_{\mathrm{W}}/\rho_{\mathrm{f}}\right)^2\right]^{1/3}$

Gradients and differences

$(\mathrm{d}p/\mathrm{d}z)$ Pressure gradient (N/m²m)
$(\mathrm{d}p/\mathrm{d}z\ F)$ Pressure gradient due to friction (N/m²m)
$(\mathrm{d}p/\mathrm{d}z\ a)$ Pressure gradient due to acceleration (N/m²m)
$(\mathrm{d}p/\mathrm{d}z\ z)$ Pressure gradient due to static head (N/m²m)

Subscripts

A   Air
c   Convective
exp   Experimental value
f   Saturated liquid
g   Saturated vapor

i	Inner tube
fo	Liquid only
nb	Nucleate boiling
nbc	Nucleate boiling contribution
o	Outer tube
pb	Pool boiling
pred	Predicted value
red	Reduced
sat	Saturation
sc	Subcooled
t	Turbulent flow
tp	Two-phase
v	Laminar flow
W	Water
w	Wall

8. References

Ali, M. I., Sadatomi, M. and Kawaji, M., 1993, "Two-phase flow in narrow channels between two flat plates", Can. J. Chem. Eng. 71, pp. 657-666.

Baker, O., 1954, "Design of pipe lines for simultaneous flow of oil and gas", Oil and Gas J. July, 26.

Baroczy, C. J., 1963, "Correlation of liquid fraction in two-phase flow with application to liquid metals", NAA-SR-8171. Fluid Sci. 28;111-121.

Premoli, A., Francesco, D., Prina, A., 1971, "A dimensionless correlation for determining the density of two-phase mixtures", Lo Termotecnica 25;17-26.

Shah, M. M., 1988, "Chart correlation for saturated boiling heat transfer: equations and further study", ASHRAE Trans 2673;185-196.

Smith, S. L., 1969, "Void fractions in two phase flow: a correlation based upon an equal velocity head model", Proc. Inst. Mech. Engrs, London 184;647–657 Part 1.

Steiner, D., 1993, "Heat transfer to boiling saturated liquids", VDI-Wärmeatlas (VDI Heat Atlas), Verein Deutcher Ingenieure, ed., VDI-Gessellschaft Verfahrenstechnik und Chemieinge- nieurwesen (GCV), Düsseldorf, Germany, (J.W. Fullarton, translator). Bao, Z. Y., Fletcher, D. F., Haynes, B. S., 2000, "Flow boiling heat transfer of freon R11 and HCFC123 in narrow passages", Int. J. Heat and Mass Transfer 43;3347-3358.

Beattie, D. R. H. and Whalley, P. B., 1982, "A simple two-phase flow frictional pressure drop calculation method", Int. J. Multiphase Flow 8;83-87.

Chang, S. D. and Ro, S. T., 1996, "Pressure Drop of Pure HFC Refrigerants and Their Mixtures Flowing in Capillary Tubes", Int J. Multiphase Flow 22(3); 551-561.

Chang Y. J., Chiang S. K., Chung T. W., Wang C. C., 2000, "Two-phase frictional characteristics of R-410A and air-water in a 5 mm smooth tube", ASHRAE Trans; DA-00-11-3;792-797.

Chen I. Y., Yang K. S., Chang Y. J., Wang C. C., 2001, "Two-phase pressure drop of air-water and R-410A in small horizontal tubes", Int. J. Multiphase Flow 27;1293-1299.

Chen, J. C., 1966, "A correlation for boiling heat transfer to saturated fluids in convective flow", Industrial and Engineering Chemistry, Process Design and Development 5;322-329.

Chisholm, D., 1967, "A theoretical basis for the Lockhart-Martinelli correlation for two-phase flow", Int. J. Heat Mass Transfer 10;1767-1778.

Chisholm, D., 1972, "An equation for velocity ratio in two-phase flow", NEL Report 535.

Chisholm, D., 1968, "The influence of mass velocity on friction pressure gradients during steam-water flow", Paper 35 presented at Thermodynamics and Fluid Mechanics Convention, Institutes of Mechanical Engineers (Bristol), March.

Chisholm, D., 1983, "Two-phase flow in pipelines and heat exchangers", New York: Longman.

Chisholm, D. and Sutherland, L. A., 1969, "Predicted of pressure gradients in pipeline systems during two-phase flow", Paper 4 presented at Symposium on Fluid Mechanics and Measurements in Two-phase Flow Systems, Leeds, 24-25, September.

Cho, J. M. and Kim, M. S., 2007, "Experimental studies on the evaporative heat transfer and pressure drop of CO_2 in smooth and micro-fin tubes of the diameters of 5 and 9.52 mm", Int. J. Refrigeration 30;986-994.

Cicchitti, A., Lombardi, C., Silvestri, M., Solddaini, G., Zavalluilli, R., 1960, "Two-phase cooling experiments— Pressure drop, heat transfer and burnout measurement", Energia Nucl 7(6);407-425.

Choi K-I A.S. Pamitran, Chun-Young Oh, Jong-Taek Oh, 2007, "Boiling heat transfer of R-22, R-134a, and CO_2 in horizontal smooth minichannels", Int. J. of Refrigeration, Vol. 30, 1336-1346.

Choi K-I, A. S. Pamitran, Chun-Young Oh, Jong-Taek Oh, 2008 "Two-phase pressure drop of R-410A in horizontal smooth minichannels", Int. J. of Refrigeration, Vol. 31, 119-129.

Choi K-I. A.S. Pamitran, Jong-Taek Oh, 2007, "Two-phase flow heat transfer of CO_2 vaporization in smooth horizontal Minichannels", Int. J. of Refrigeration, vol. 30, 767-777.

Choi K-I. A.S. Pamitran, Jong-Taek Oh, Kiyoshi Saito, 2009, "Pressure drop and heat transfer during two-phase flow vaporization of propane in horizontal smooth minichannels", Int. J. of Refrigeration, vol. 32, 837-845.

Cooper, M. G., 1984, "Heat flow rates in saturated nucleate pool boiling–a wide-ranging examination using reduced properties", In: Advances in Heat Transfer. Academic Press 16;157-239.

Dittus, F. W. and Boelter, L. M. K., 1930, "Heat transfer in automobile radiators of the tubular type", University of California Publication in Engineering 2;443-461.

Dukler, A. E., Wicks, I. I. I. M., Cleveland, R. G., 1964, "Pressure drop and hold-up in two-phase flow", AIChE J. 10(1);38-51.

Friedel, L., 1979, "Improved friction pressure drop correlations for horizontal and vertical two-phase pipe flow", Presented at the European Two-phase Flow Group Meeting, Ispra, Italy, Paper E2, June.

Gnielinski, V., 1976, "New equations for heat and mass transfer in turbulent pipe and channel flow", International Chemical Engineering 16: 359-368

Grönnerud, R., 1979, "Investigation of Liquid Hold-Up, Flow-Resistance and Heat Transfer in Circulation Type Evaporators", Part IV: Two-phase flow resistance in boiling refrigerants, Annexe 1972-1, Bull. de l'Inst. du Froid, International Inst. of Refrigeration, Paris.

Gungor, K. E., Winterton, H. S., 1987, "Simplified General Correlation for Saturated Flow Boiling and Comparisons of Correlations with Data", Chem.Eng.Res 65; 148-156.

Jung, D., Kim, Y., Ko, Y., Song, K., 2003, "Nucleate boiling heat transfer coefficients of pure halogenated refrigerants", Int. J. Refrigeration 26;240-248.

Jung, D. S., McLinden, M., Radermacher, R., Didion, D., 1989, "A Study of Flow Boiling Heat Transfer with Refrigerant Mixtures", Int J. Mass Transfer 32(9);1751-1764.

Kandlikar, S. G., 1990, "A general correlation for saturated two-phase flow boiling heat transfer inside horizontal and vertical tubes", Journal of Heat Transfer 112;219-228.

Kandlikar, S. G., 2002, "Fundamental issues related to flow boiling in minichannels and microchannels", Experimental Thermal and Fluid Science 26;389-407.

Kattan N., 1996, "Contribution to the heat transfer analysis of substitute refrigerants in evaporator tubes with smooth or enhanced tube surfaces", PhD thesis No 1498, Swiss Federal Institute of Technology, Lausanne, Switzerland.

Kattan, N., Thome, J. R., Favrat, D., 1998, "Flow boiling in horizontal tubes: part 1 – development of a diabatic two-phase flow pattern map", J. Heat Transfer 120;140-147.

Kawahara, A., Chung, P. M. Y., Kawaji, M., 2002, "Investigation of two-phase flow pattern, void fraction and pressure drop in a microchannel", Int J. of Multiphase Flow 28;1411-1435.

Kew, P. A., Cornwell, K., 1997, "Correlations for the Prediction of Boiling Heat Transfer in Small-Diameter Channels", Applied Thermal Engineering 17(8-10);705-715.

Kuo, C. S. and Wang C. C., 1996, "In-tube evaporation of HCFC-22 in a 9.52 mm micro-fin/smooth tube", Int. J. Heat Mass Transfer 39;2559-2569.

Lazarek, G. M. and Black, S. H., 1982, "Evaporative heat transfer, pressure drop and critical heat flux in a small diameter vertical tube with R-113", Int. J. Heat Mass Transfer 25;945-960.

Lockhart, R. W. and Martinelli, R. C., 1949, "Proposed correlation of data for isothermal two-phase, two-component flow in pipes", Chem. Eng. Prog. 45;39-48.

McAdams, W. H., 1954, "Heat transmission", third ed. New York: McGraw-Hill.

Mishima, K. and Hibiki, T., 1996, "Some characteristics of air-water two-phase flow in small diameter vertical tubes", Int. J. Multiphase Flow 22;703-712.

Müller-Steinhagen, H. and Heck, K., 1986, "A simple friction pressure drop correlation for two-phase flow in pipes", Chemical Engineering and Processing 20(6);297-308

Oh, H. K., Ku, H. G., Roh, G. S., Son, C. H., Park, S. J., 2008, "Flow boiling heat transfer characteristics of carbon dioxide in a horizontal tube", Applied Thermal Engineering 28;1022-1030.

Ould Didi, M. B., Kattan, N., Thome, J. R., 2002, Prediction of Two-phase Pressure Gradients of Refrigerants in Horizontal Tubes, Int J. Refrig. 25;935-947.

Pamitran A.S, Kwang-Il Choi, Jong-Taek Oh, Hoo-Kyu Oh, 2008, "Two-phase pressure drop during CO2 vaporization in horizontal smooth minichannels" Int. J. of Refrigeration, Vol. 31, 1375–1383.

Pamitran A.S. Kwang-Il Choi, Jong-Taek Oh, Hoo-Kyu Oh, 2007, "Forced convective boiling heat transfer of R-410A in horizontal minichannels", Int. J. of Refrigeration, Vol. 30,155-165.

Pamitran A.S. Kwang-Il Choi, Jong-Taek Oh, Pega Hrnjak., 2010, "Characteristics of two-phase flow pattern transitions and pressure drop of five refrigerants in horizontal circular small tubes", Int. J. of Refrigeration, vol. 33, 578-588.

Park, C. Y. and Hrnjak, P. S., 2007, "CO2 and R410A flow boiling heat transfer, pressure drop, and flow pattern at low temperatures in a horizontal smooth tube", Int. J. Refrigeration 30;166-178.

Peng, X. F. and Peterson, G. P., 1996, "Forced convective heat transfer of single-phase binary mixtures through microchannels", Experimental Thermal and Fluid Science 12;98-104.

Petukhov, B. S. and Popov, V. N., 1963, "Theoretical calculation of heat exchanger in turbulent flow in tubes of an incompressible fluid with variable physical properties", High Temp. 1(1);69-83.

Pettersen, J., 2004, "Flow vaporization of CO_2 in microchannels tubes", Exp. Therm.

Tran, T. N., Chyu, M. C., Wambsganss, M. W., France, D. M., 2000, "Two-phase pressure drop of refrigerants during flow boiling in small channels: An experimental investigation and correlation development", Int. J. Multiphase Flow 26;1739-1754.

Tran, T. N., Wambsganss, M. W., France, D. M., 1996, "Small circular- and rectangular-channel boiling with two refrigerants", Int. J. Multiphase Flow 22(3);485-498.

Wambsganss, M. W., France, D. M., Jendrzejczyk, J. A., Tran, T. N., 1993, "Boiling Heat Transfer in a Horizontal Small-diameter Tube", AMSE Trans 115;963-975.

Wang, C. C., Chiang, C. S., Lu, D. C., 1997, "Visual observation of two-phase flow pattern of R-22, R-134a, and R-407C in a 6.5-mm smooth tube", Exp. Therm. Fluid Sci. 15;395-405.

Wojtan, L., Ursenbacher, T., Thome, J. R., 2005, "Investigation of flow boiling in horizontal tubes: part I – a new diabatic two-phase flow pattern map", Int. J. Heat Mass Transfer 48;2955-2969.

Wattelat, J. P., Chato, J. C., Souza, A. L., Christoffersen, B. R., 1994, "Evaporative Characteristics of R-12, R-134a, and a Mixture at Low Mass Fluxes", ASHRAE Trans 94-2-1;603-615.

Yan, Y. Y., Lin, T. F., 1998, "Evaporation Heat Transfer and Pressure Drop of Refrigerant R-134a in a Small Pipe", Int J. of Heat and Mass Transfer 41;4183-4194.

Yang, C. Y. and Lin, T. Y., 2007, "Heat transfer characteristics of water flow in microtubes", Experimental Thermal and Fluid Science 32(2);432-439.

Yoon, S. H., Cho, E. S., Hwang, Y. W., Kim, M. S., Min, K., Kim, Y., 2004, "Characteristics of evaporative heat transfer and pressure drop of carbon dioxide and correlation development", Int. J. Refrigeration 27;111-119.

Yu, W., France, D. M., Wambsganss, M. W., Hull, J. R., 2002, "Two-phase Pressure Drop, Boiling Heat Transfer, and Critical Heat Flux to Water in a Small-diameter Horizontal Tube", Int J. of Multiphase Flow 28;927-941.

Yun, R., Kim, Y., Kim, M. S., 2005, "Convective boiling heat transfer characteristics of CO_2 in microchannels", Int. J. Heat. Mass Transfer 48;235-242.

Zhang, L., Hihara, E., Saito, T., Oh, J. T., 1997, "Boiling Heat Transfer of a Ternary Refrigerant Mixture inside a Horizontal Smooth Tube", Int J. Mass Transfer 40(9);2009-2017.

Zhang, M. and Webb, R. L., 2001, "Correlation of two-phase friction for refrigerants in small-diameter tubes", Experimental Thermal and Fluid Science 25;131-139.

Zhang, W., Hibiki, T., Mishima, K., 2004, "Correlation for flow boiling heat transfer in mini-channels", Int. J. Heat and Mass Transfer 47;5749-5763.

Zhao, Y., Molki, M., Ohadi, M. M., Dessiatoun, S. V., 2000, "Flow boiling of CO_2 in microchannels", ASHRAE Trans DA-00-2-1;437-445.

Zivi, S. M., 1964, "Estimation of Steady-State Steam Void-Fraction by Means of the Principle of Minimum Entropy Generation", J. Heat Transfer 86;247-252.
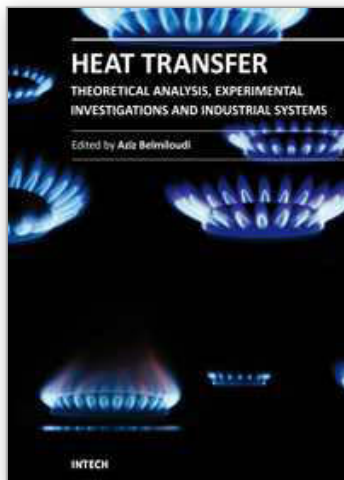
Heat Transfer - Theoretical Analysis, Experimental Investigations and Industrial Systems

Edited by Prof. Aziz Belmiloudi

ISBN 978-953-307-226-5

Hard cover, 654 pages

Publisher InTech

Published online 28, January, 2011

Published in print edition January, 2011

Over the past few decades there has been a prolific increase in research and development in area of heat transfer, heat exchangers and their associated technologies. This book is a collection of current research in the above mentioned areas and discusses experimental, theoretical and calculation approaches and industrial utilizations with modern ideas and methods to study heat transfer for single and multiphase systems. The topics considered include various basic concepts of heat transfer, the fundamental modes of heat transfer (namely conduction, convection and radiation), thermophysical properties, condensation, boiling, freezing, innovative experiments, measurement analysis, theoretical models and simulations, with many real-world problems and important modern applications. The book is divided in four sections : "Heat Transfer in Micro Systems", "Boiling, Freezing and Condensation Heat Transfer", "Heat Transfer and its Assessment", "Heat Transfer Calculations", and each section discusses a wide variety of techniques, methods and applications in accordance with the subjects. The combination of theoretical and experimental investigations with many important practical applications of current interest will make this book of interest to researchers, scientists, engineers and graduate students, who make use of experimental and theoretical investigations, assessment and enhancement techniques in this multidisciplinary field as well as to researchers in mathematical modelling, computer simulations and information sciences, who make use of experimental and theoretical investigations as a means of critical assessment of models and results derived from advanced numerical simulations and improvement of the developed models and numerical methods.

How to reference

In order to correctly reference this scholarly work, feel free to copy and paste the following:

INTECH
open science | open minds

InTech Europe

University Campus STeP Ri

InTech China

Unit 405, Office Block, Hotel Equatorial Shanghai